

---

Masters Theses

Student Theses and Dissertations

---

1965

## Active band-pass filters using twin-tee networks

Terry B. Watson

Follow this and additional works at: [https://scholarsmine.mst.edu/masters\\_theses](https://scholarsmine.mst.edu/masters_theses)



Part of the [Electrical and Computer Engineering Commons](#)

Department:

---

### Recommended Citation

Watson, Terry B., "Active band-pass filters using twin-tee networks" (1965). *Masters Theses*. 6687.  
[https://scholarsmine.mst.edu/masters\\_theses/6687](https://scholarsmine.mst.edu/masters_theses/6687)

This thesis is brought to you by Scholars' Mine, a service of the Missouri S&T Library and Learning Resources. This work is protected by U. S. Copyright Law. Unauthorized use including reproduction for redistribution requires the permission of the copyright holder. For more information, please contact [scholarsmine@mst.edu](mailto:scholarsmine@mst.edu).

T1760

ACTIVE BAND-PASS FILTERS USING TWIN-TEE NETWORKS

BY

TERRY B. WATSON

72 P

A

THESIS

submitted to the faculty of the  
UNIVERSITY OF MISSOURI AT ROLLA

in partial fulfillment of the requirements for the

Degree of

MASTER OF SCIENCE IN ELECTRICAL ENGINEERING

Rolla, Missouri

1965

Approved by

R. D. DeWoody (advisor)

J. H. Charnock

J. L. Zepkin

C. A. Johnson

113162

## ABSTRACT

The primary objective of this thesis was the design and construction of a set of filters to determine the spectral energy density of random signal data in the spectrum from 10 cps to 20 kcps. The statement of the problem placed rather exacting conditions on the cost and performance of the equipment, and these conditions were met to the extent detailed in the following pages.

A secondary objective was the investigation of techniques to improve the performance of band-pass active filters using resistive-capacitive feedback networks. This objective was not achieved to the author's satisfaction, although several promising ideas were discovered.

## ACKNOWLEDGEMENTS

The author wishes to thank his advisor Mr. R. T. Dewoody for the assistance given on this thesis. Much appreciation is also due to Mr. O. S. Anderson and Mr. Dick Schroder for their help in constructing and testing the equipment.

## TABLE OF CONTENTS

ABSTRACT . . . . .	11
ACKNOWLEDGES . . . . .	111
LIST OF FIGURES . . . . .	vi
LIST OF SYMBOLS . . . . .	viii
CHAPTER	
I.    STATEMENT OF THE PROBLEM . . . . .	1
II.   AN INTRODUCTION TO THE THEORY OF ACTIVE BAND-PASS FILTERS USING TWIN-TEE NETWORKS. .	7
A.   Analysis of Single Stage . . . . .	7
B.   Cascaded Stages . . . . .	10
III.  DESIGN AND CONSTRUCTION OF THE EQUIPMENT . .	15
A.   Design of Amplifier Circuits . . . . .	15
B.   Selection of Components for the Twin-Tee Filters and Design Details Involving the Twin-Tee Filters . . . . .	18
C.   Construction of Equipment . . . . .	20
IV.   EQUIPMENT PERFORMANCE . . . . .	24
A.   Comparison of the Performance with the Specifications. . . . .	24
B.   Suggestion for Improvement . . . . .	25
V.   OTHER DEVELOPMENTAL WORK . . . . .	30
A.   Transistorization of the Equipment . .	31
B.   Subtraction of Signals Output from Two Parallel Filter Stages . . . . .	31
C.   Cascaded Stages Using Feed-Forward Techniques . . . . .	34
D.   Variations of the Twin-Tee Network . .	35

APPENDIX		
I.	THE TWIN-TEE FILTER . . . . .	37
A.	Basic Theory . . . . .	37
B.	Tuning Twin-Tee Filters to Obtain a Specified Null at a Specified Frequency.	42
II.	OPERATING, MODIFICATION, AND MAINTAINANCE INSTRUCTIONS . . . . .	49
A.	Operating Instructions . . . . .	49
B.	Modification of the Equipment . . . . .	50
C.	Maintainance . . . . .	51
III.	DEFINITION OF BANDWIDTHS . . . . .	68
END NOTES	. . . . .	71
VITA	. . . . .	72

## LIST OF FIGURES

Figures	Page
1. Block diagram of a single-stage active filter . . .	8
2. Magnitude of $\bar{E}_0/\bar{E}_1$ for $\bar{A} = 10, 20, \text{ and } 50$ . . . . .	11
3. Phase angle of $\bar{E}_0/\bar{E}_1$ for $\bar{A} = 10, 20, \text{ and } 50$ . . . . .	12
4. Individual and overall frequency response curves for three cascaded stages . . . . .	14
5. A circuit of a single-stage active filter . . . . .	15
6. An external view of the equipment . . . . .	21
7. A view of the equipment with the front panel removed . . . . .	22
8. A view of a filter rack . . . . .	23
9. Frequency response curves for decade 1 . . . . .	26
10. Frequency response curves for decade 2 . . . . .	27
11. Frequency response curves for decade 3 . . . . .	28
12. Frequency response curves for decade 4 . . . . .	29
13. Block diagram of a circuit for subtracting the outputs of two parallel active filters . . . . .	32
14. Frequency response of the circuit in Figure 13 . . .	33
15. A filter using feed-forward . . . . .	34
16. Diagram of a twin-tee filter with the output and common terminals interchanged . . . . .	35
17. The twin-tee filter . . . . .	37
18. Frequency characteristics of a twin-tee filter . . .	41
19. Circuit for tuning twin-tee filters . . . . .	43
20. Construction of the twin-tee filter boards . . . . .	46
21. A circuit for tuning twin-tee filters after installation . . . . .	47

Figures	Page
22. Modification for larger input signals . . . . .	50
23. Schematic diagram of the amplifier circuits . . . . .	53
24. Rear view of the amplifier rack . . . . .	54
25. Schematic diagram of the power supply . . . . .	55
26. Front view of the amplifier rack . . . . .	59
27. Rear view of a connector plug and wiring details .	60



## LIST OF SYMBOLS

$\bar{E}_1$  = Input voltage to the active filter.

$\bar{E}_0$  = Output voltage of the active filter.

$\bar{\beta}$  = Voltage transfer characteristic of a resistive-capacitive network.

$\omega$  = Angular frequency.

$\omega_0$  = Null angular frequency for a twin-tee filter.

$\rho = \omega / \omega_0$

$\bar{A}$  = Voltage gain of an amplifier.

$f_n$  = Critical (lower-edge, band-center, or upper-edge) frequency of a band-pass filter.

$k\Omega$  = Kiloohm.

$m\Omega$  = Megohm.

## I. STATEMENT OF THE PROBLEM

The equipment which forms the subject of this thesis is intended for application in a study of turbulent liquid flow. For this reason, the discussion will refer to this field for the explanation of the equipment's theory and operation, although the equipment could be applied to any other process having signals within the range of the equipment.

In investigations of random processes, such as turbulent liquid flow, several methods are used to determine the character of the process in question. By character of the process, one refers to such quantities as magnitude and periodicity of the process. It is known the energy losses in a turbulent flow stream are dependent upon the average fluid velocity and the magnitude and periodicity of the turbulence, but the process is not fully understood.<sup>1\*</sup>

It is thought that energy losses due to turbulence occur in the following manner. Energy is transferred from the flow stream to the liquid particles on the boundary of an eddy. These particles then transfer the energy to faster moving liquid particles on the boundaries of smaller eddies. The process continues to still smaller eddies with larger fluid particle velocities, until the energy is actually lost due to shearing of the liquid. Magnitudes and frequencies may

\*Subscripts refer to the End Notes.

be assigned to the velocities of the fluid particles and the regularity with which these velocities occur. A knowledge of the magnitude and frequency distribution of the particle velocities inside the eddies would lead to a better understanding of turbulence. This desired information is generally known as the spectral energy density<sup>2</sup> and is to be determined by the equipment described in this thesis. The objective of the equipment's application is to determine the effects of the fluid temperature, the average fluid velocity, and the fluid properties (or composition) upon the spectral energy density of the turbulence and the resulting energy losses.

The equipment is to be used to analyze signals obtained with a hot-wire anemometer. The operation of this anemometer is as follows. A small metallic wire is placed in the liquid flow stream and an electric current is passed through the wire, causing a heating of the wire. If the liquid flow is laminar, the temperature (and resistance) of the wire reaches an equilibrium value. If the liquid flow is turbulent, the temperature (and resistance) of the wire increases or decreases, according to the instantaneous flow of liquid over the wire. By means of suitable calibration, this variation of the wire's resistance appears as an electrical signal corresponding to the turbulence of the flow stream. This type of anemometer has an upper frequency limit of approximately 100 cycles per seconds and more sophisticated circuitry is used to obtain a response up to 150 kc. The reader is referred

to the literature for a more detailed discussion of hot-wire anemometers.<sup>3</sup>

The electrical signal obtained with the hot-wire anemometer may be processed to determine the spectral energy density of the liquid turbulence. At least three methods are available for performing this analysis. These methods are: (1) by the autocorrelation function, (2) by the power density spectrum, and (3) by an appropriate function of the second probability distribution.<sup>4</sup> The first two of these methods will be used by the recipients of the equipment, and the results of the two methods will be compared for agreement.

In the first method, the autocorrelation function of the signal is determined and the Fourier transform of the autocorrelation function yields the spectral energy density.

In the second method, the signal is processed by passing it through a wave analyzer to an averaging circuit to a magnitude detector.<sup>5</sup> In this case, the wave analyzer consists of band-pass frequency filters. Frequency-band analysis, rather than single-frequency analysis, is used for the following reasons. First, the analysis is performed much quicker with band-analysis as fewer measurements are required. Second, the energy content of a frequency band is greater than the energy level for a single frequency inside that band, and the ratio of the signal magnitude to the noise generated by the processing equipment is increased (and improved). The averaging circuit is required because the signal is random

and the magnitude will vary with time. Such parameters as fluid temperature, average fluid velocity, and fluid composition will be held constant and the turbulence should be a stationary random process.<sup>6</sup> In such a process, the analysis of signals over one time interval should give results very similar to the results of analysis over another time interval. The averaging circuit provides a more constant signal level for measurement. The averaging circuit and the magnitude detector are combined in a thermocouple rms voltmeter. The signal power is used to heat a thermocouple which supplies power for the deflection of the voltmeter needle. The averaging process results from the thermal mass of the thermocouple.

The voltmeter readings are then squared and divided by the respective frequency bandwidths ( $\Delta f$  in cps). The resulting numbers are then plotted as points ( $E^2/\Delta f$  versus frequency  $f$ ) at the center frequencies of the respective bands. This plot of points is actually the spectral power density, but is sometimes referred to as the spectral energy density. For white noise (noise with a constant power density spectrum<sup>7</sup>), the plot of points would form a straight line. This method of measuring the spectral power (or energy) density is far faster than the first method which requires finding the Fourier transform of the autocorrelation function of the signal.

This thesis is concerned with the design and construction of the wave analyzer equipment. The following equipment

specifications were requested:

(1) that a set of band-pass filters be provided to cover the frequency spectrum from 10 cps to 20,000 cps in bandwidths of one-third frequency octave. For reasons to be discussed later, an equivalent bandwidth of one-tenth decade was delivered. Appendix III contains a discussion of how these bandwidths are defined.

(2) that the filters be linear.

(3) that the noise level of the filters should not be greater than that of the anemometer (0.45 mv for 1 kc bandwidth or 0.9 mv for 5 kc bandwidth<sup>8</sup>).

(4) that the filter responses should be relatively sharp. This specification was not specifically defined, as the equipment users will use several techniques to compensate for the differences between the actual band-pass frequency responses and the ideal rectangular band-pass frequency response. In an attempt to define a figure of merit for filter sharpness, it was requested that the power level of the total signal should be within 10 percent of the sum of the power levels for the individual frequency bands.

(5) that the total cost of the filters should be relatively small.

The first three requirements might be satisfied with commercially available passive filters, but the fourth and fifth specifications restricted the choice of solutions to that of active filters. The desired frequency spectrum con-

sists of 34 bands, and the cost of this many passive inductive-capacitive filters would have been prohibitive, especially for the frequencies less than approximately 200 cps. Passive resistive-capacitive filters might have been used, but the size and cost would have been excessive if the fourth specification was satisfied. Thus, economic considerations ruled out the use of passive filters and it was necessary to resort to active filters. The following sections are devoted to the theory, design, construction, and performance of one type of active band-pass filter.

## II. AN INTRODUCTION TO THE THEORY OF ACTIVE BAND-PASS FILTERS USING TWIN-TEE NETWORKS

### A. ANALYSIS OF A SINGLE STAGE

In applications such as this where it is desired to process signals with frequencies in the audio spectrum, passive band-pass filters with good frequency responses are relatively expensive. Fortunately, it is possible to obtain quite satisfactory band-pass filters by the use of a few amplifiers and relatively inexpensive resistive-capacitive networks in feedback circuits.

A good deal of work has been done in this section of the field of active filters and parts of the following discussion are quite similar to the development found in the literature.<sup>9,10</sup> Somewhat different notation was used in the two sources and the most significant differences are noted below.

The basic idea of these active filters involves the use of frequency-selective networks in feedback circuits to obtain a desired (band-pass) frequency response. The principle of operation may be explained by referring to the circuit of Figure 1.



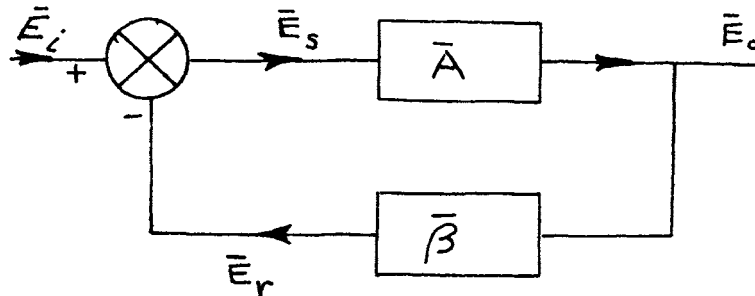


Figure 1. Block diagram of a single-stage active filter.

It can be shown that

$$\frac{\bar{E}_o}{\bar{E}_i} = \frac{\bar{A}}{1 + \bar{\beta} \bar{A}} \quad (1)$$

where  $\bar{A} = \bar{E}_o/\bar{E}_1$  is the voltage gain of an amplifier and  $\bar{\beta} = \bar{E}_r/\bar{E}_o$  is the voltage transfer characteristic of a frequency-selective network. Several types of networks have been used as the  $\bar{\beta}$  network,<sup>11</sup> but the author obtained the most satisfactory results with the twin-tee (or parallel-tee) filter. This filter has a voltage transfer characteristic

$$\bar{\beta} = \frac{1 - \rho^2}{1 - \rho^2 + j4\rho} \quad (2)$$

where  $\rho = f/f_0^*$  and  $f_0$  is the null frequency of the filter. Note that  $\bar{\beta} = 0$  for  $f = f_0$  and  $\bar{\beta}$  approaches unity for very small and large values of frequency. A derivation of Eq. 2

\* The notation above is that used by Valley and Wallman. Seeley used  $\Omega = \rho - j\rho$ .

and other properties of the twin-tee filter may be found in Appendix I.

If the  $\bar{\beta}$  of Eq. 2 is substituted into Eq. 1, one obtains

$$\frac{\bar{E}_o}{\bar{E}_i} = \frac{\bar{A}}{1 + \frac{\bar{A}(1-\rho^2)}{1-\rho^2 + j4\rho}} \quad (3)$$

$$\frac{\bar{E}_o}{\bar{E}_i} = \frac{\bar{A}(1-\rho^2 + j4\rho)}{(1+\bar{A})(1-\rho^2) + j4\rho} \quad (4)$$

For  $f = f_0$  or  $\rho = 1$ , note that

$$\frac{\bar{E}_o}{\bar{E}_i} = \bar{A} \quad (5)$$

For frequencies very much larger or smaller than  $f_0$ ,

$$\frac{\bar{E}_o}{\bar{E}_i} \doteq \frac{\bar{A}}{1 + \bar{A}} \quad (6)$$

Thus this circuit acts as a band-pass filter in that the ratio of the output voltage to the input voltage varies with frequency, reaching a maximum at the frequency  $f_0$ . In circuits of this type, the filter action results from frequency-selective amplification, rather than the frequency-selective attenuation of passive filters. Note in Eqs. 5 and 6 that the selectivity of the filter is dependent upon the amplifier gain  $\bar{A}$ . Figure 2 shows the variation of the magnitude of  $\bar{E}_o/\bar{E}_i$  with frequency for amplifier voltage gains of

10, 20, and 50. Figure 3 shows the phase angle of the output voltage, relative to the input, for these same values of  $\bar{A}$ . Note that the frequency responses shown in Figure 2 are quite similar to those of inductive-capacitive filters with different values of  $Q$ . One may exploit this similarity and show that<sup>12</sup>

$$Q \doteq \frac{|\bar{A}|}{4} \quad (7)$$

#### B. CASCADED STAGES

Since the frequency response of the system in Figure 1 is approximately that of a single-tuned filter, it is necessary to cascade two or more stages to obtain the desired band-pass frequency response. For this equipment, three cascaded stages were required to meet the specifications. Figure 4 shows the frequency responses of the three stages separately and the overall cascaded response. The data for Figure 4 was obtained by measurement of the actual equipment response.

The first stage was tuned to the lower band-edge frequency of 282 cps, the second stage was tuned to the band-center frequency of 316 cps, and the third stage was tuned to the upper band-edge frequency of 355 cps. To obtain a better approximation to the ideal rectangular band-pass frequency response with cascaded stages, it is necessary to have a smaller voltage gain and selectivity in the band-center stage than in the band-edge stages.<sup>13</sup>

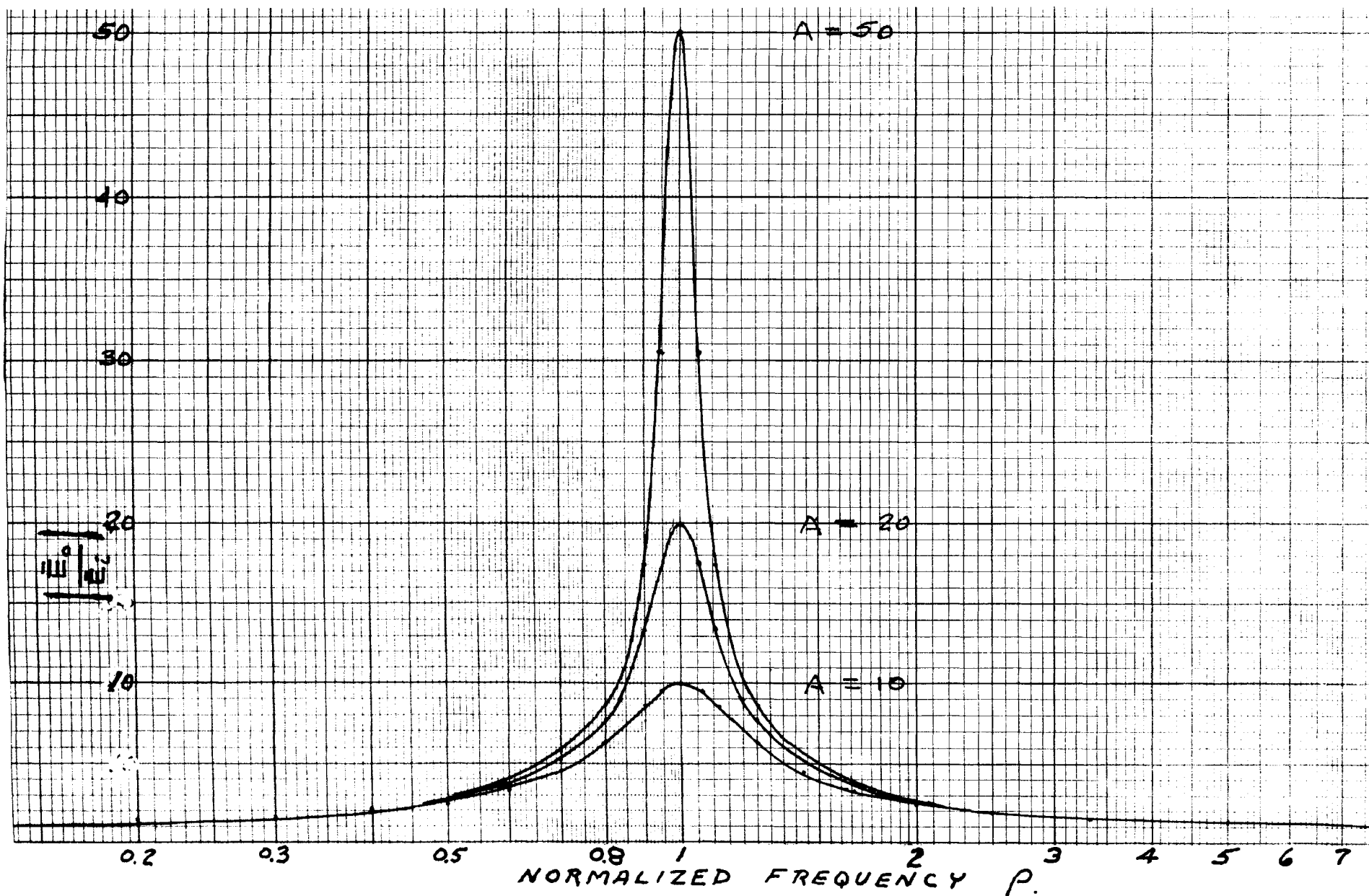


FIGURE 2. MAGNITUDE OF  $\vec{E}_0/\vec{E}_i$  FOR  $A = 10, 20, \text{ AND } 50.$

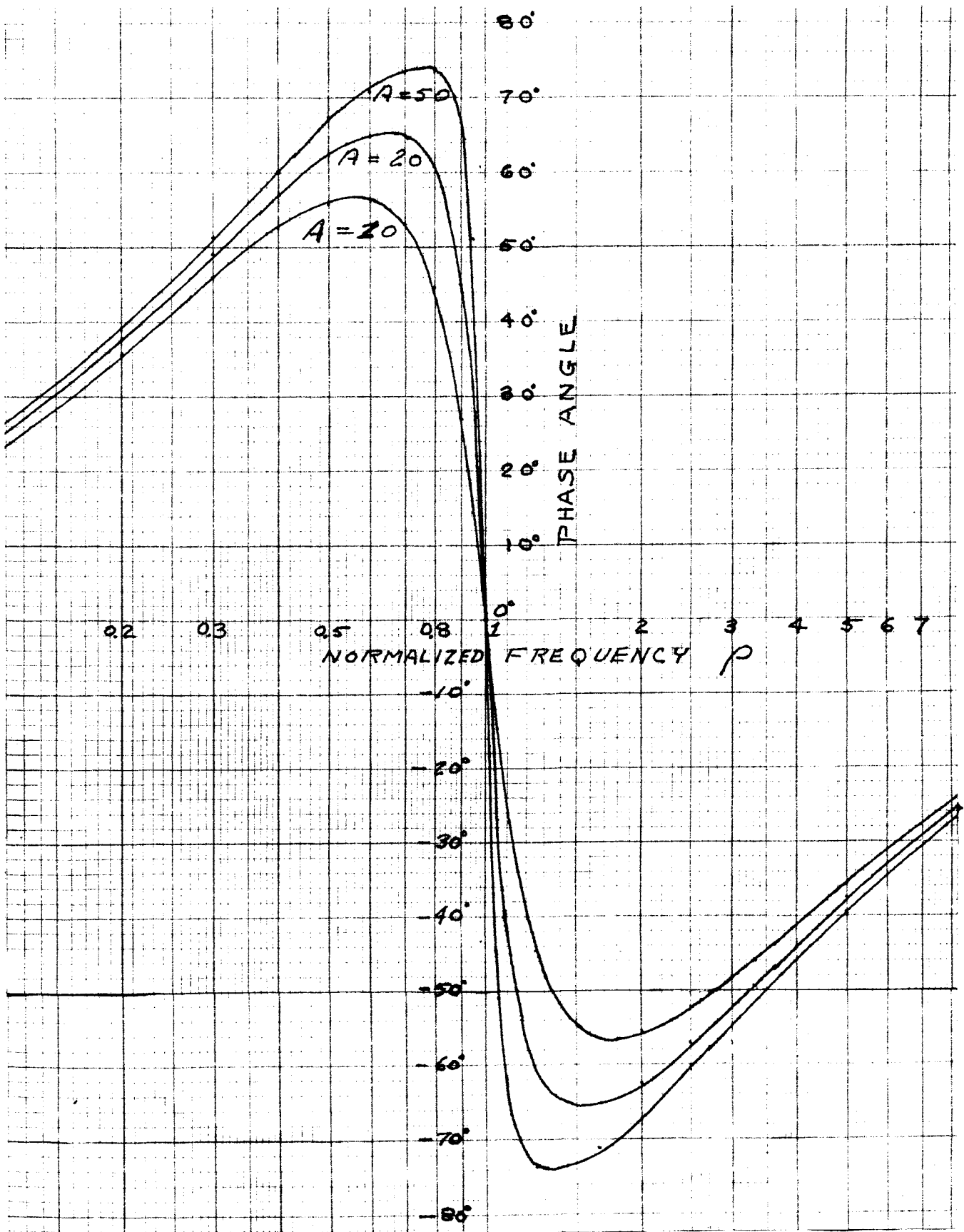


FIGURE 3. PHASE ANGLE OF  $\frac{E_0}{E_1}$  FOR  $A=10, 20,$  AND  $50$ .

In Figure 4, it can be seen that the voltage gain of the second stage is approximately one-half that of the voltage gain for the first and third stages.

Appendix III contains a discussion of how the critical (band-center and band-edge) frequencies are selected.

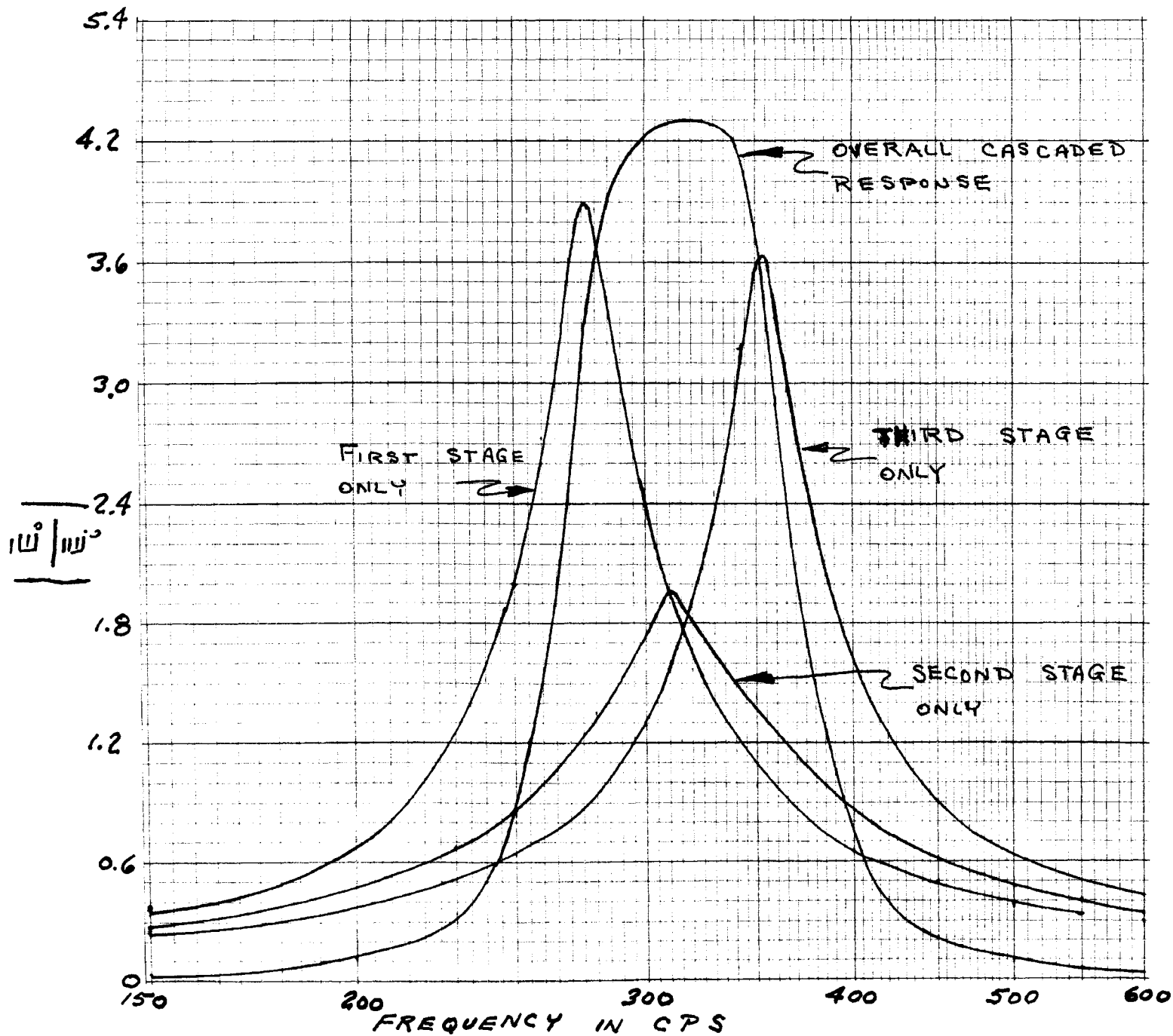


FIGURE 4. INDIVIDUAL AND OVERALL FREQUENCY RESPONSE CURVES FOR THREE CASCADED STAGES.

### III. DESIGN AND CONSTRUCTION OF THE EQUIPMENT

#### A. DESIGN OF THE AMPLIFIER CIRCUITS

Several circuits are available for performing the desired signal amplification and subtraction,<sup>14</sup> but the circuit of Figure 5 was chosen for the following reasons. This circuit has a large input impedance, requires a moderate plate supply voltage, allows self-bias operation, and has sufficient voltage gain to obtain the desired sharpness or selectivity. The actual circuit, with component values, is shown in Appendix II.

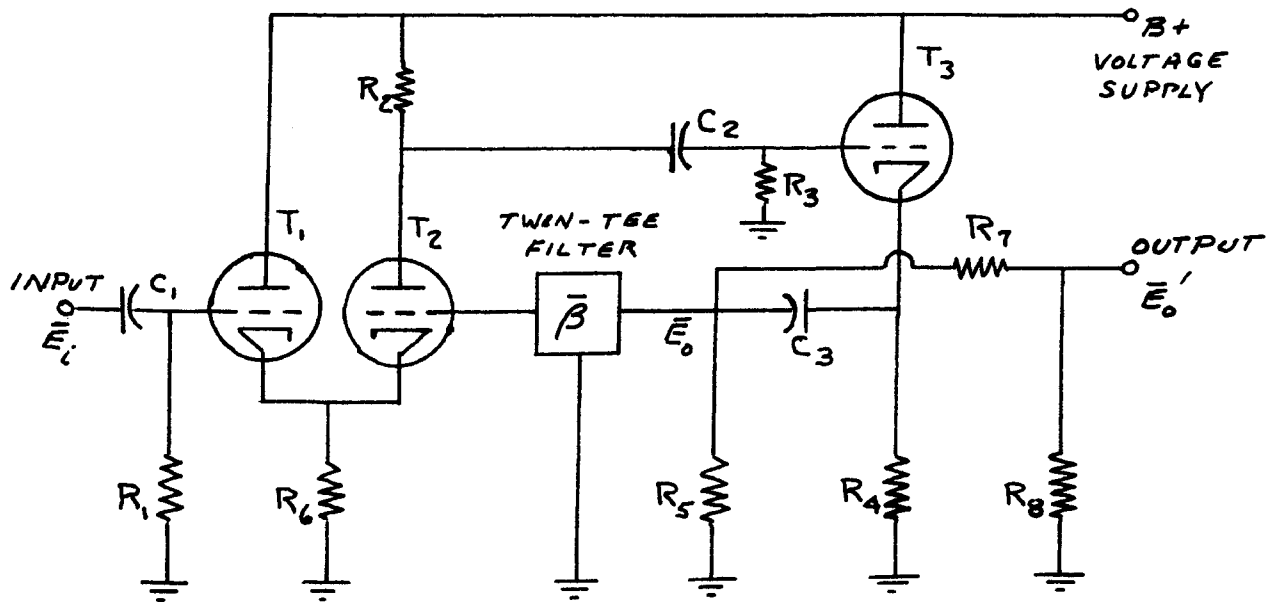


Figure 5. A circuit of a single-stage active filter.



The operation of the circuit is as follows, Triodes  $T_1$  and  $T_2$  form a difference amplifier, with  $\bar{\beta} \bar{E}_0$  being subtracted from  $\bar{E}_{in}$  by the grid of  $T_2$ . The 12AX7 dual triode was selected for  $T_1$  and  $T_2$  as this tube offers a large voltage gain with low noise. Premium grade tubes were specified for the original installation and for future replacements. This provides greater reliability and less change in the performance of the equipment when these vacuum tubes are replaced. The triodes were biased (see Figure 23) to allow operation in a more linear region of the tube characteristics<sup>15</sup> and provide a voltage gain of approximately 40 in the first and third stages. The voltage gain of the second stage is approximately 20 (see section B of Chapter II).

The cathode follower, using one unit of a 6SN7 dual triode for  $T_3$ , was added to provide isolation between the plate of  $T_2$  and the input terminals of the twin-tee filter. The input impedance of the twin-tee filter (see Appendix I) is small enough to cause a large reduction in voltage gain if the input terminal of the filter is connected to the plate of  $T_2$ . The cathode follower circuit, with its high input impedance and low output impedance, minimizes the effects of the input impedance of the twin-tee filter.

Note that the grid-leakage resistance for  $T_2$  ( $R_5$ ) is placed on the input terminals of the twin-tee filter, rather than on the output terminals at the grid of  $T_2$ . There is a D.C. path between the input and output terminals

of the filter and hence a D.C. path from the grid of  $T_2$  to ground. This allows the output terminals of the twin-tee filter to be connected to the grid of  $T_2$ , which is essentially an open circuit (except for the wiring capacitance and the input capacitance of  $T_2$  which are discussed below). This open-circuit load for the twin-tee filter results in a sharper frequency response (see Appendix I for the output impedance of a twin-tee filter and the effect of a load impedance).

In order to obtain a sharp frequency response, the voltage gain of each stage should be as large as possible, but not so large as to cause the output of one stage to saturate the following stage. To overcome this conflict between sharpness and linear operation, a voltage-divider consisting of resistances  $R_7$  and  $R_8$  was used to reduce the magnitude of the output signal of each stage before applying this signal to the input of the following stage. This does not reduce the frequency selectivity of the stage since

$$\frac{\bar{E}_o}{\bar{E}_i} = \frac{\bar{A}}{1 + \beta \bar{A}} \quad (8)$$

and the actual output of the stage is

$$\bar{E}_o' = \bar{E}_o \frac{R_8}{R_7 + R_8} \quad (9)$$

Since the attenuation of the voltage-divider is not frequency dependent, a larger voltage gain may be used to obtain

greater frequency selectivity without also over-driving the following stage.

#### B. SELECTION OF COMPONENTS FOR THE TWIN-TEE FILTERS AND DESIGN DETAILS INVOLVING THE TWIN-TEE FILTERS

Several factors had to be considered when selecting component values to obtain twin-tee filters with null frequencies at the desired values. The most important economic consideration involved the use of the smallest number of available standard-value components with the maximum allowable tolerance. Another most important factor was the interaction between the filter and the rest of the circuit, namely the effects of the input and output impedance of a twin-tee filter.

In a compromise between cost and accuracy, it was decided to use components with a 5% tolerance. A technique in Appendix I was devised to compensate for component value variations.

In Table 1 of Appendix III, the ratio of each critical frequency to the next lowest critical frequency is approximately 1.12. It was decided to use resistances of 24, 27, and 30 units since  $27/24 = 1.13$  and  $30/27 = 1.11$ . For a trio of critical frequencies, the capacitance was chosen to obtain a null at the center frequency with a resistance of 27 units. The same capacitance and a resistance of 30 units was used to obtain a null at the lower critical frequency. The same capacitance and a resistance of 24 units was used for the filter at the upper critical frequency of the trio. For another trio of critical frequencies, another value of capacitance

and the same resistance values were used. This simplified the selection of components and allowed a cost reduction due to quantity purchases. The previously mentioned method of compensation was then used to obtain filters with the desired attenuation and frequency accuracy.

The selection of the actual resistance and capacitance values was influenced by the values of capacitance in the amplifier circuits and their effect on the overall frequency response of the equipment. At the upper frequency limit of 22.4 kc, it was desired that the output impedance of the twin-tee filters should be less than half the load impedance presented by the connecting cables and the grid of the amplifier tube (70  $\mu\mu f$  due to the cable and 120  $\mu\mu f$  due to the Miller effect occurring at the grid of the tube). To satisfy this condition on the output impedance, resistances of 24 k $\Omega$ , 27 k $\Omega$ , and 30 k $\Omega$  were used for the filters with frequencies between 700 cps and 22.4 kc. For frequencies less than 700 cps, resistances of 240 k $\Omega$ , 270 k $\Omega$ , and 300 k $\Omega$  were used in the filters. This allowed the use of smaller capacitors in the filters and in the coupling networks ( $C_3$  in Figure 5).

Molded-carbon resistors and polystyrene-dielectric capacitors were used, since the desired values were available at a reasonable price. Both of these component materials have negative temperature coefficients, and the null frequencies of the filters will change with large temperature changes. To date, no significant temperature effects have been observed.

The possibility of temperature effects could have been reduced had mica or mylar capacitors (with positive temperature coefficients) been available.

It is expected the filters' null frequencies and degree of attenuation will be quite stable, as the components are subjected to only relatively small signal voltages.

During the experimental work, it was found that the overall response is most dependent upon the accuracy of the null frequencies and the degree of attenuation in the different twin-tee filters. It was found that a frequency accuracy of 1% was satisfactory. Quite uniform responses were obtained if the attenuation of each twin-tee filter was between minus 65 db and 60 db (1.6 to 1.0 mv output for 1 volt input) at the null frequency.

### C. CONSTRUCTION OF THE EQUIPMENT

In the preliminary discussions of the equipment specifications, it was also desired that the equipment could be operated and repaired by persons with a minimum of instruction. This objective of simplicity had a large influence upon the method of construction used for this equipment.

Figure 6 shows a front view of the equipment. All of the controls are mounted on the front panel and are labelled to reduce any confusion as to the operation of the equipment. The operating instructions are given in Appendix II.

Figure 7 shows a view of the equipment with the front panel removed.

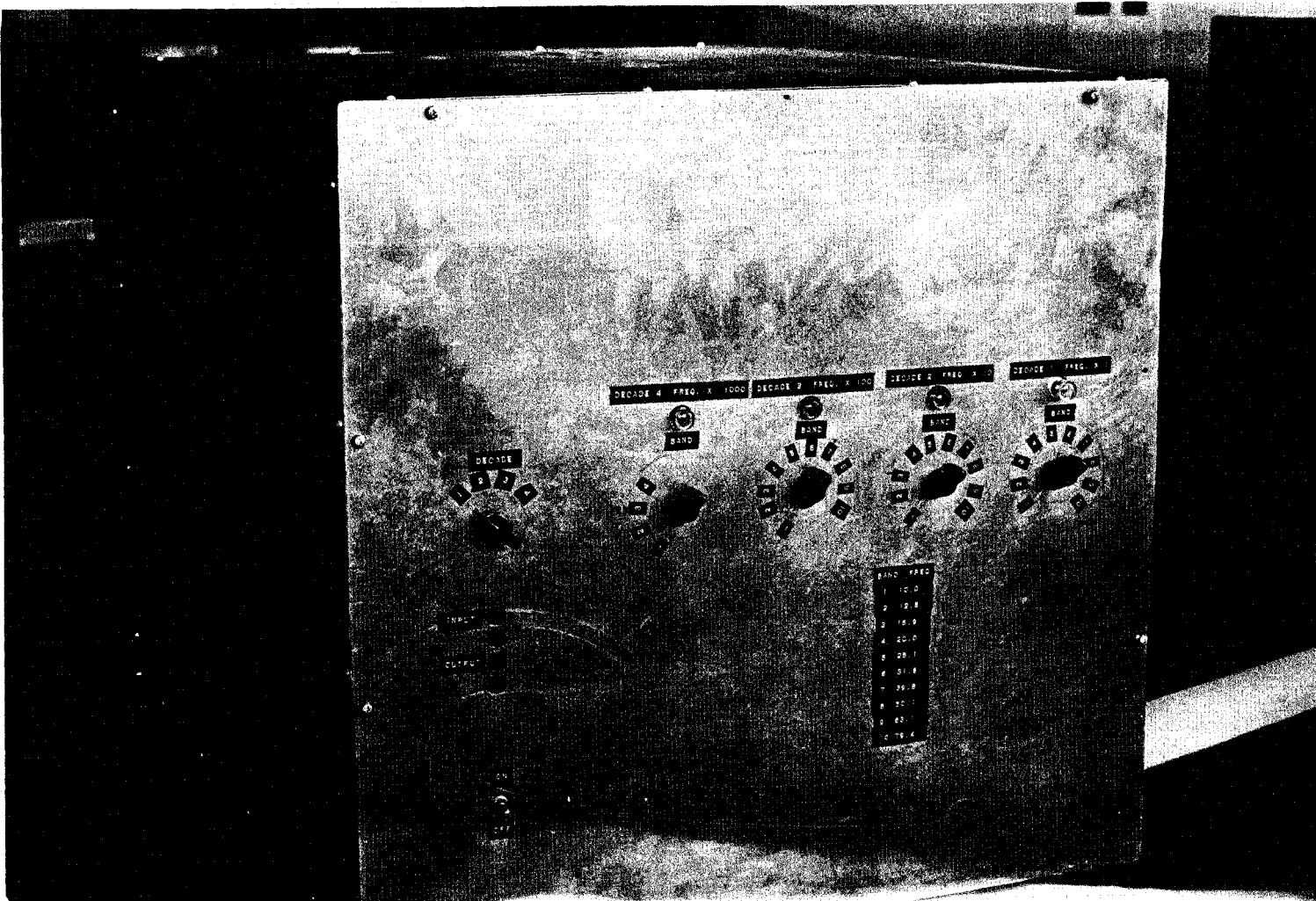


Figure 6. An external view of the equipment.

The amplifiers, the power supply, and the decade switch (used to select the frequency decade of interest) are mounted on the rack at the left.

The remaining four racks support the twin-tee filters and the band switches for the four frequency ranges or decades.

Figure 8 shows one rack partially removed from the box.

Low capacitance coaxial cable (RG-62/U with  $13.5 \mu\mu f$  per foot) was used for all connections on and between the racks to provide a small, predictable wiring capacitance.

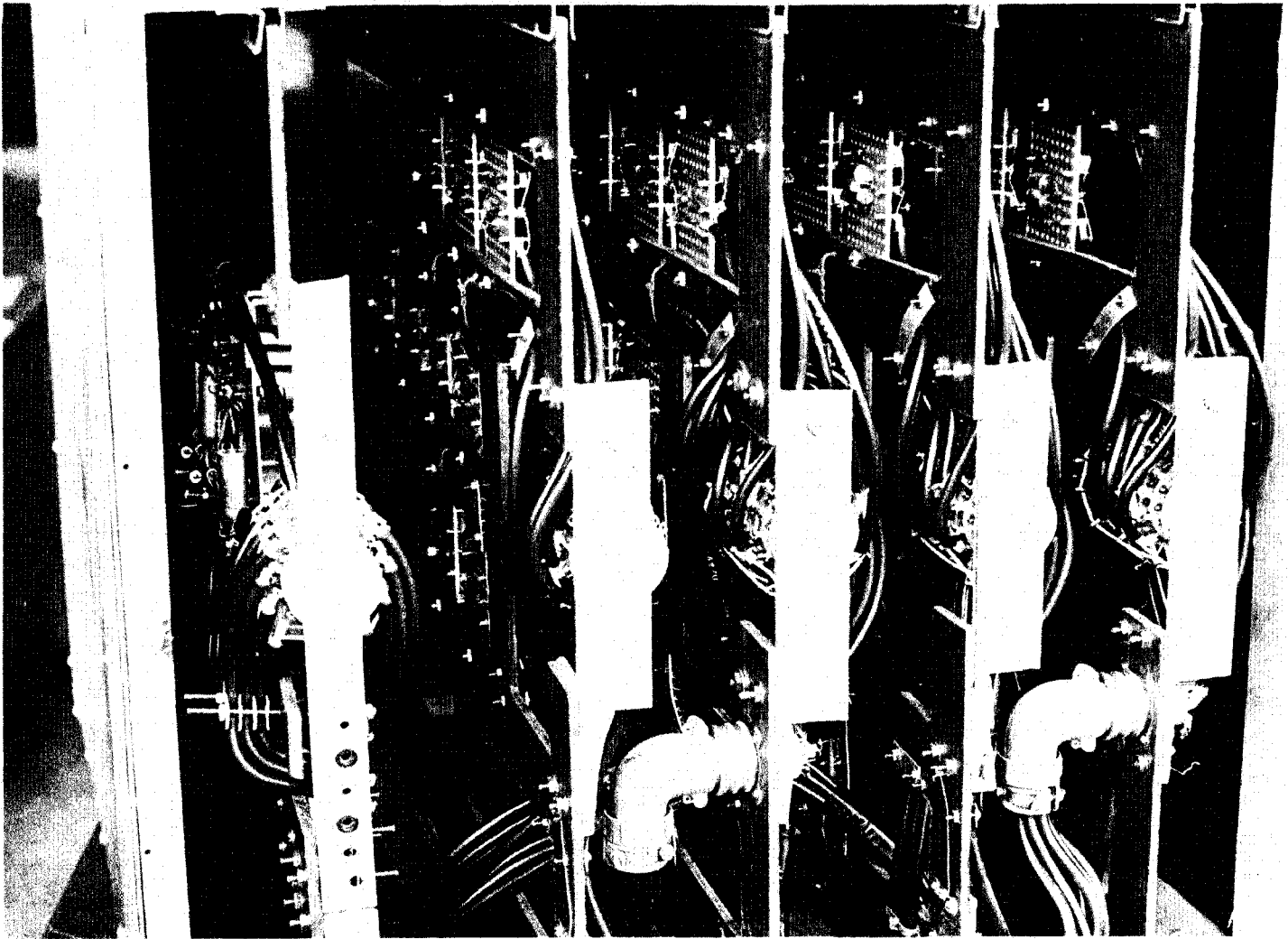


Figure 7. A view of the equipment with the front panel removed.

The filter racks for the higher frequencies were placed closer to the amplifier rack, as shorter connecting cables have less wiring capacitance.

Connectors were placed in the rack-to-rack connecting cables to allow the removal and repair of any rack if needed.

The reader is referred to section C of Appendix II for additional information pertaining to the construction of the equipment.

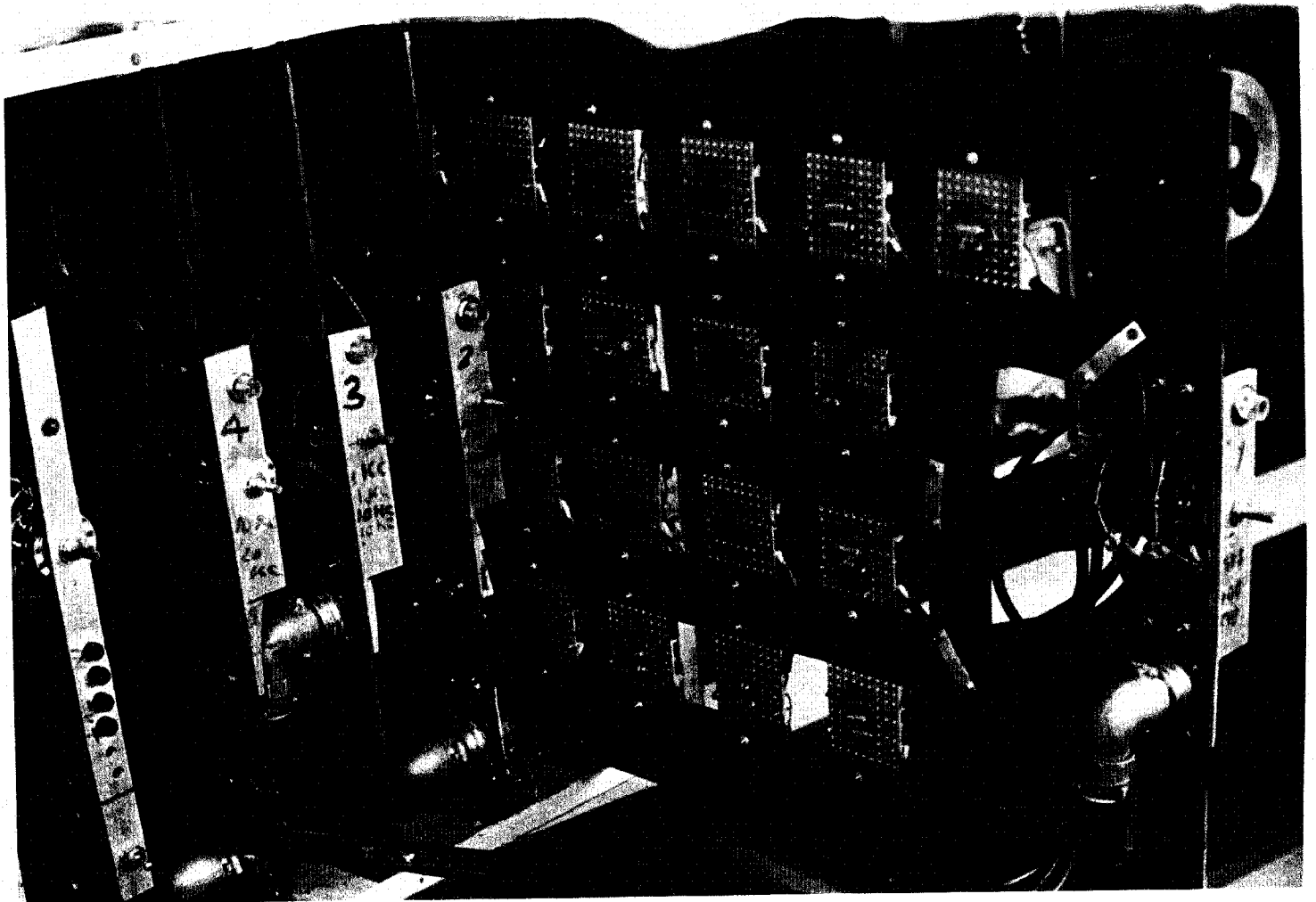


Figure 8. A view of a filter rack.



## IV. EQUIPMENT PERFORMANCE

### A. COMPARISON OF THE PERFORMANCE WITH THE SPECIFICATIONS

The equipment specifications are given in Chapter I and will be treated in the order shown there.

1. Figures 9, 10, 11, and 12 show the frequency responses of the equipment for the four frequency ranges. Several of the response curves leave a good deal to be desired regarding symmetry about the band-center frequency and uniformity in the maximum values of  $\bar{E}_0/\bar{E}_1$ . Section B of this chapter contains several suggestions for improving the symmetry and uniformity of maximum magnitudes.

2. For the present application, the total input signal will be less than 400 millivolts. The equipment will perform with no measureable distortion for input signals having no more than 200 millivolts in any one frequency band.

3. With the input terminals short-circuited, the output voltage is 0.2 millivolts on all bands except the 100 cps and 126 cps band. The output voltage is 1.2 mv and 2.2 mv on the 100 and 126 cps bands respectively. The frequency of this increased noise is 120 cps and is most probably due to the second harmonic of the 60 cps cathode-heater supply. This

noise could be reduced by using D.C. power for the cathode-heaters, but this cannot be justified.

4. At the time of this writing, the equipment had not been put to use. For lack of another suitable signal source, the specification concerning filter sharpness could not be tested. At half and twice the center frequency of each band, the relative attenuation is at least minus 40 db (1/100).

5. The total cost of the parts in the equipment is less than one-fourth the cost of passive filters to cover the same frequency spectrum. No estimate of the labor cost can be made as a large part of the required time was spent on efforts that did not directly contribute to the final result.

#### B. SUGGESTIONS FOR IMPROVEMENT

It is the author's opinion that the lack of symmetry and uniformity for several of the frequency-response curves is due to unbalanced twin-tee filters. This opinion is based upon the observation that the frequency response of a band did not vary more than a few percent when amplifier vacuum tubes were interchanged. The performance could be improved by using the second method of Appendix I to tune or balance the twin-tee filters, as this method takes the characteristics of the amplifier circuits into account also.

The twin-tee filters may be tuned much more easily and accurately if a variable resistance is used for  $R_3$  in each filter.

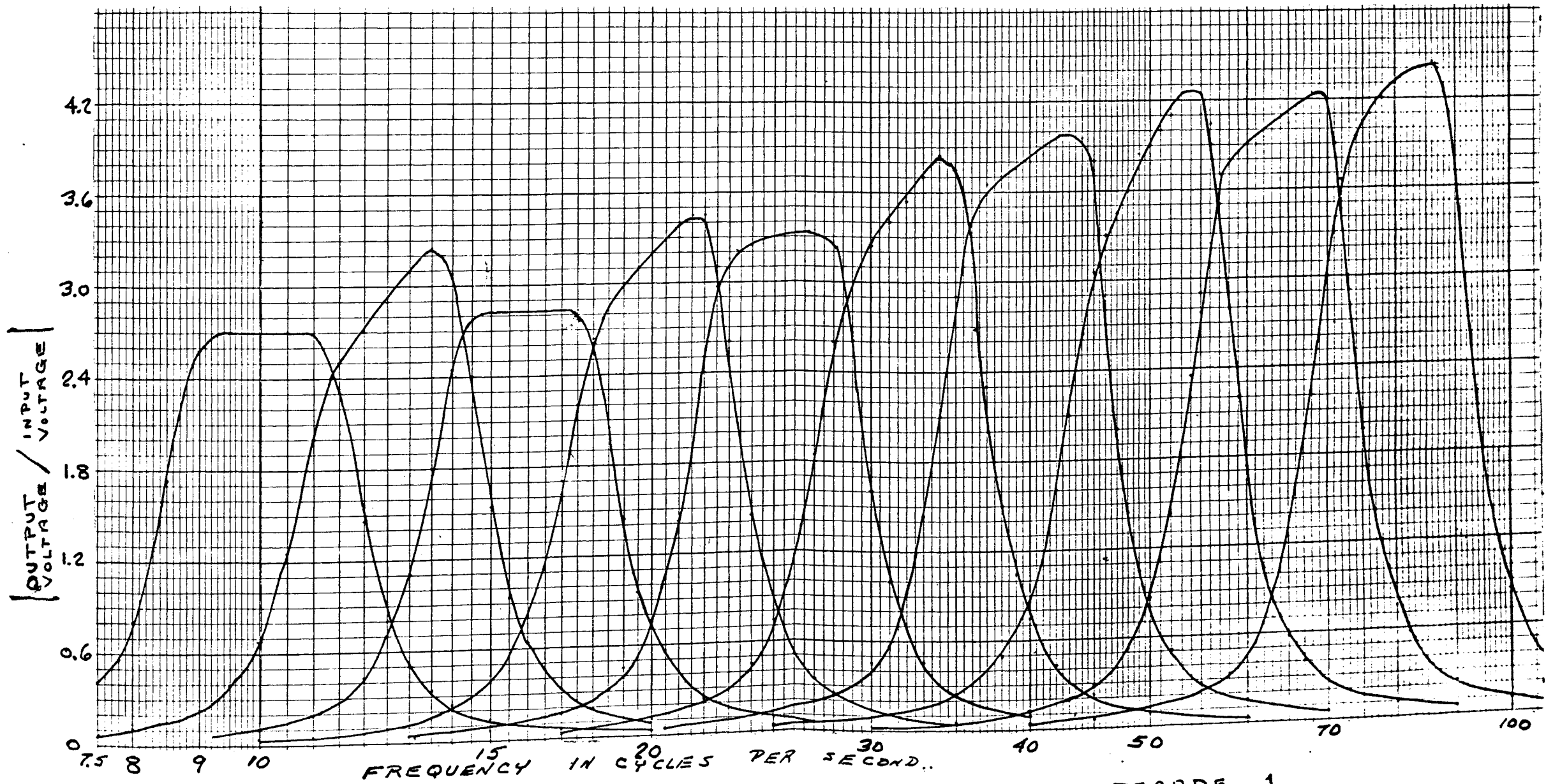


FIGURE 9. FREQUENCY RESPONSE CURVES FOR DECADE 1.

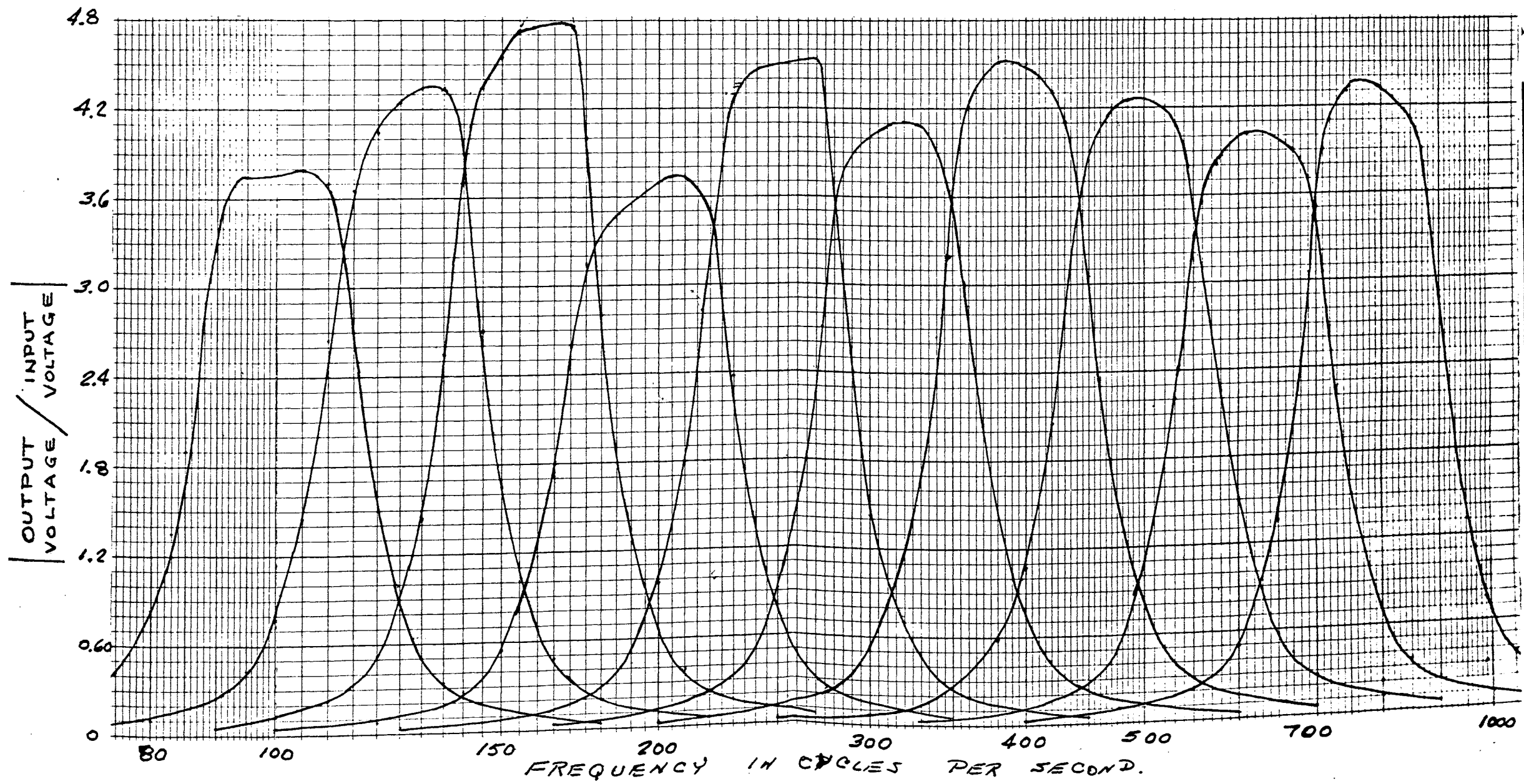


FIGURE 10. FREQUENCY RESPONSE CURVES FOR DECADE 2.

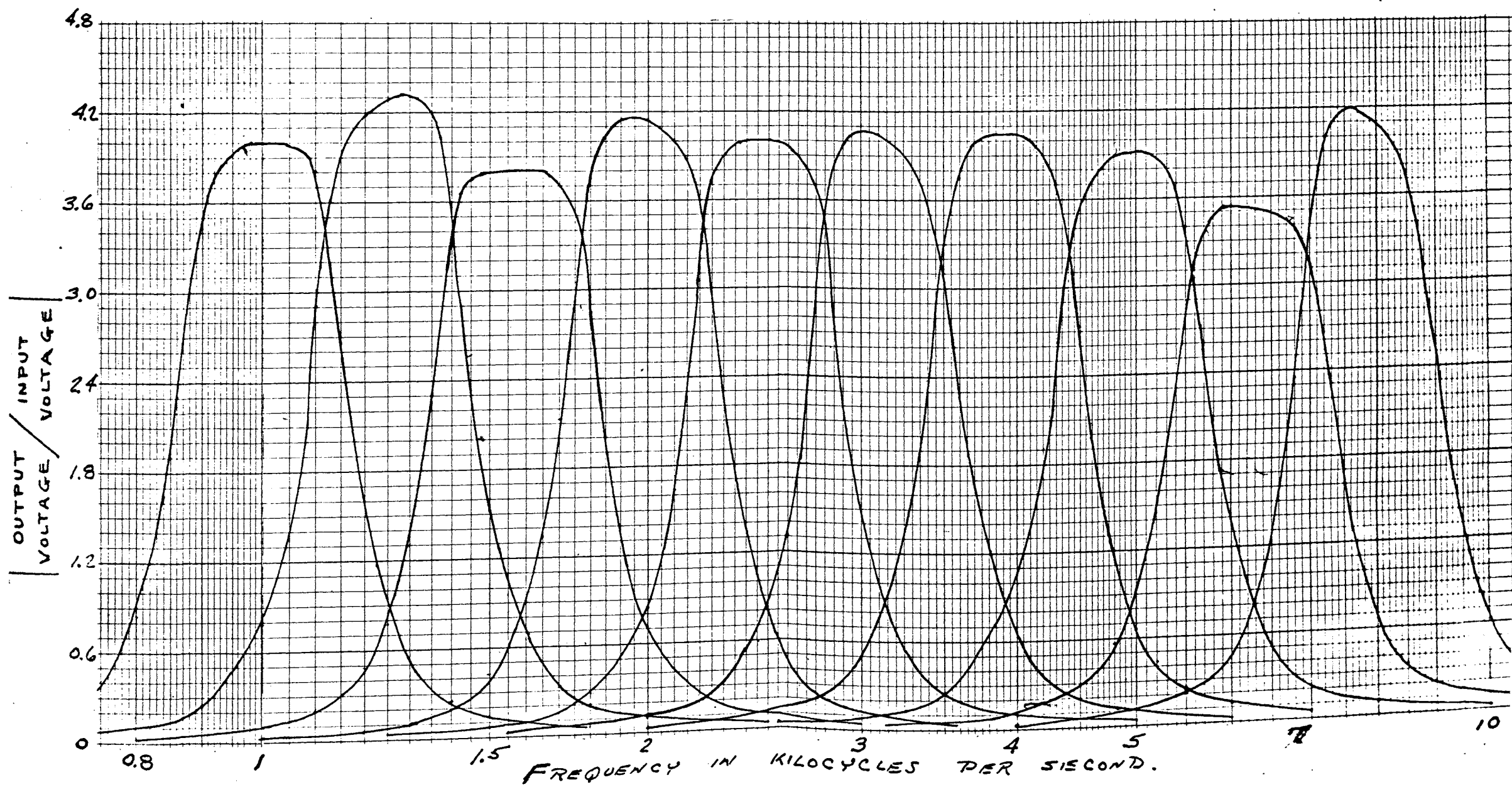


FIGURE 11. FREQUENCY RESPONSE CURVES FOR DECADE 3.

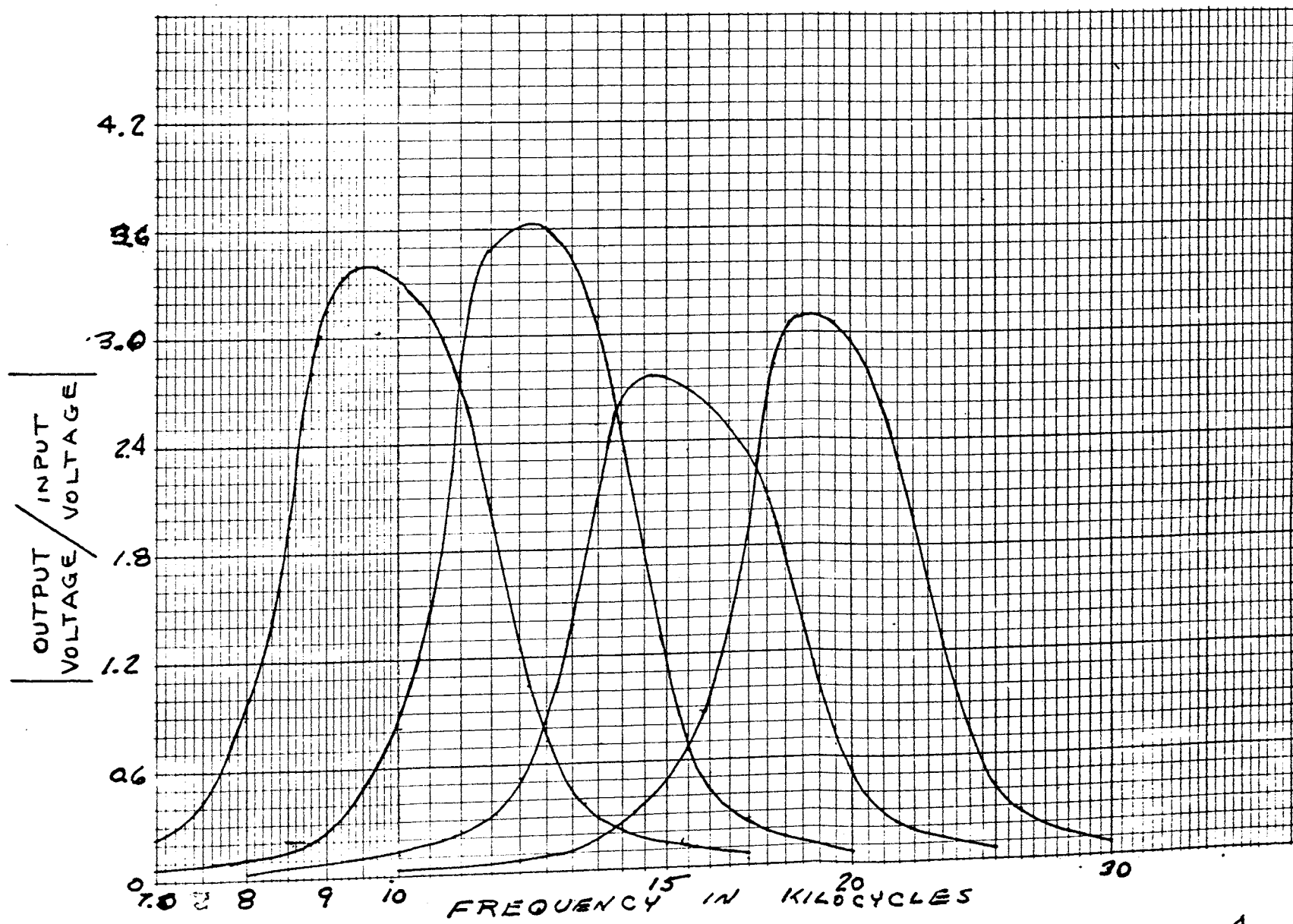


FIGURE 12. FREQUENCY RESPONSE CURVES FOR DECADE 4.

## V. OTHER DEVELOPMENTAL WORK

A large part of the time required to complete the equipment was spent on efforts which did not directly affect the final design.

First, the recipients of the equipment requested the use of transistors if possible. The use of vacuum tubes, rather than transistors, is justified below.

The secondary objective of this thesis actually arose from a misinterpretation of the specifications. A bandwidth of one-third octave was originally specified, but there was some confusion as to the exact meaning of the term third octave (see Appendix III). It was thought that desired bandwidth was such as to require eight bands per decade, rather than ten bands. Obtaining satisfactory equipment is much more difficult with a larger bandwidth.

For a filter consisting of three stages and having a relative attenuation of minus 40 db ( $1/100$ ) at half and twice the band-center frequency, a ripple of at least 15% must be tolerated with a bandwidth of one-eighth decade.

The equipment recipients later agreed to accept a bandwidth of one-tenth decade, but prior to this, a good deal of

work was done in an attempt to reduce the ripple encountered with a bandwidth of one-eighth decade. The most significant results of this work are presented below.

#### A. TRANSISTORIZATION OF THE EQUIPMENT

After a certain amount of work had been done with vacuum tubes, it was requested that transistors be used instead. It was necessary to use a Darlington transistor connection to obtain a large amplifier gain. Even with careful selection of transistors, it was not possible to obtain uniform amplification in the different stages. A second major disadvantage of transistors is their low input impedance. This input impedance would have loaded the twin-tee filter output terminals and reduced the frequency selectivity. When an emitter follower was added between the filter output and the base of the amplifying transistor (similar to  $T_2$  in Figure 5), a large increase in noise was observed. It was then decided to revert to vacuum tubes for the amplifier elements. The present cost of field effect transistors ruled out their use in this equipment.

#### B. SUBTRACTION OF OUTPUT SIGNALS FROM TWO PARALLEL FILTER STAGES

In an attempt to improve the response and use a smaller number of stages, the circuit of Figure 13 was used. The blocks labeled  $f_1$  and  $f_3$  are two separate active filters tuned to the band-edge frequencies  $f_1$  and  $f_3$ . In Figure 3 it is shown that the output of an active filter differs from the input by some phase angle as well as by magnitude. For



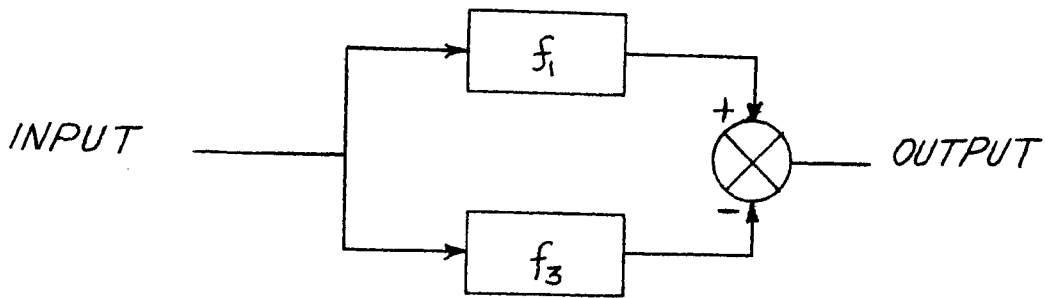


Figure 13. Block diagram of a circuit for subtracting the outputs of two parallel active filters.

frequencies above or below both  $f_1$  and  $f_3$ , the output phase angles of the two stages are of the same sign. The difference of the two signals is then less than the output of either stage separately. For frequencies in the desired band-pass region ( $f_1 < f < f_3$ ), the output angle of stage 1 is lagging ( $-90^\circ < \text{angle} < 0^\circ$ ) while the angle of stage 3 is leading ( $0 < \text{angle} < 90^\circ$ ). With the proper stage amplification and frequency separation between  $f_1$  and  $f_3$ , the difference of the two outputs is relatively large and constant in the band-pass range. This method was unsuccessful when tried with transistors and a bandwidth of one-eighth decade. Through an oversight, this method was not tried later with vacuum tubes and a bandwidth of one-tenth decade. This method, using two stages and 38 twin-tee filters rather than the three stages and 72 filters now contained in the equipment, might have been used had sufficient time been available for development. Figure 14 shows the frequency response

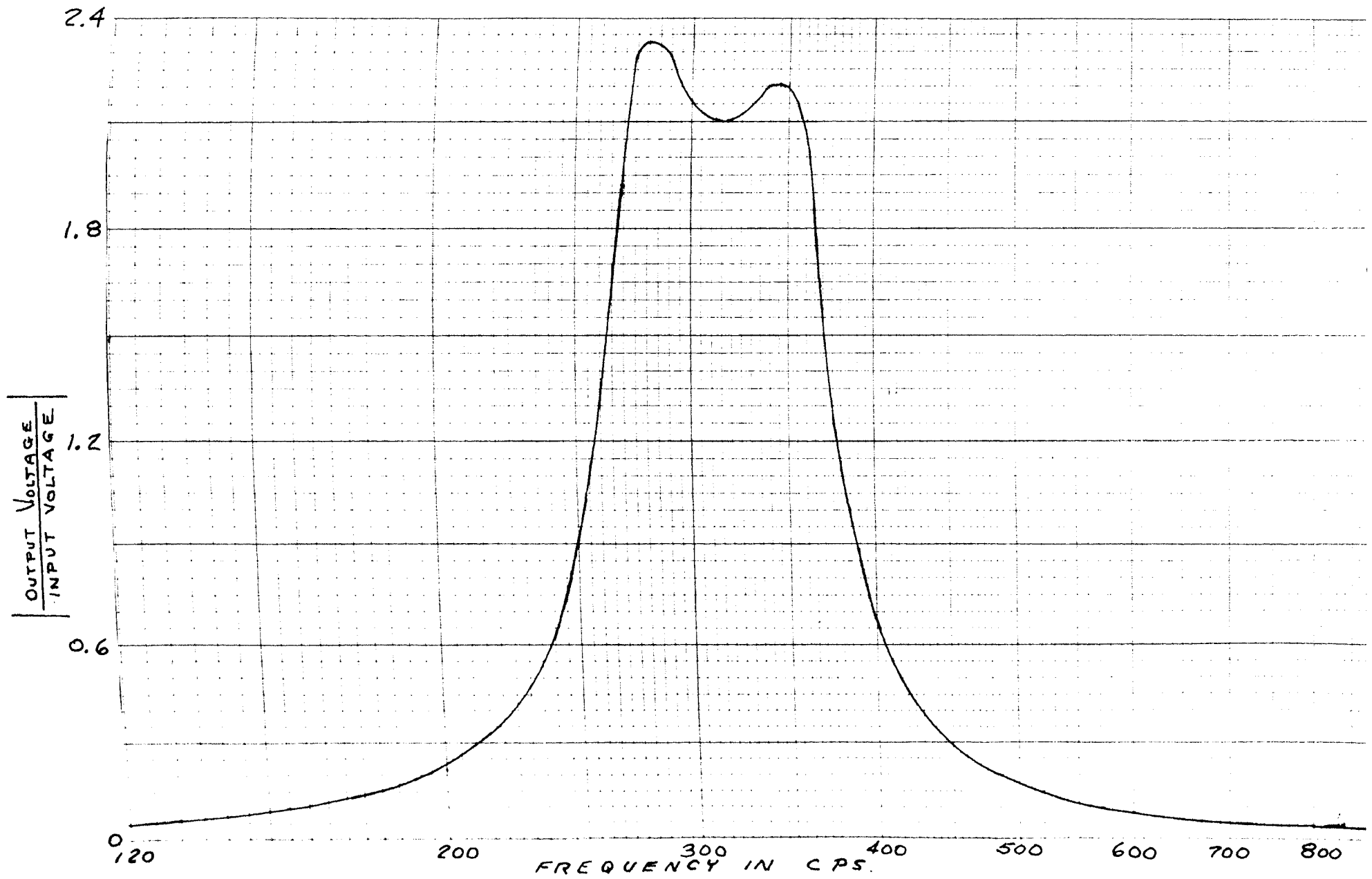


FIGURE 14 . FREQUENCY RESPONSE OF THE CIRCUIT IN FIGURE 13 WITH  $f_1 = 282$  CPS AND  $f_3 = 355$  CPS .

of such a filter. This data was obtained by using the first and third stages of the equipment, with the switches set for the 316 cps band.

### C. CASCADED STAGES USING FEED-FORWARD TECHNIQUES.

In another effort to reduce the filter ripple, the circuit of Figure 15 was tried. The blocks  $f_1$ ,  $f_2$ , and  $f_3$  are

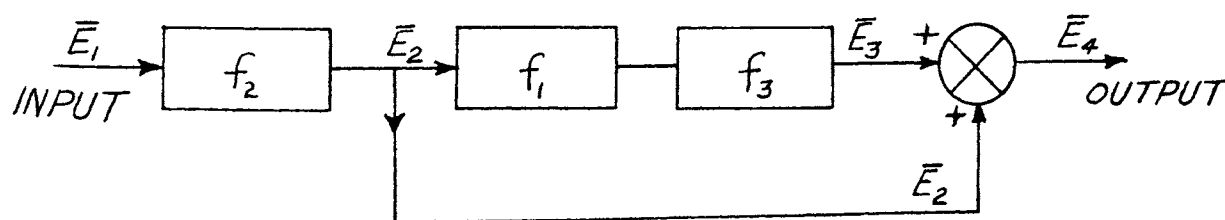


Figure 15. A filter using feed-forward.

active filter stages tuned to the lower, center, and upper critical frequencies of a desired frequency band. This circuit provides less ripple in the band-pass range and has sharper band edges than the usual cascaded connection, but the attenuation at very high and low frequencies is also reduced. This method is also dependent upon the phase shift given by each stage. For frequencies inside the band-pass range ( $f_1 < f < f_3$ ), the signals  $\bar{E}_2$  and  $\bar{E}_3$  differ by a small phase angle and the output signal  $\bar{E}_4$  is increased. For signals slightly outside the band-pass range, the signals  $\bar{E}_2$  and  $\bar{E}_3$  differ by a phase angle approaching  $180^\circ$ . The sum of the signals then results in reduced output signal  $\bar{E}_4$ . At very

large and small frequencies, the phase difference between  $\bar{E}_2$  and  $\bar{E}_3$  again approaches zero and the signal output increases. The ultimate attenuation is limited by the stage  $f_2$ . This method of signal combination was discovered just prior to the reduction of the desired bandwidth from one-eighth decade to one-tenth decade. Experimentation then showed that the above technique was not needed with the reduced bandwidth.

#### D. VARIATIONS OF THE TWIN-TEE NETWORK.

During an experimental run, the output and common leads of a twin-tee filter were reversed by mistake. This resulted in the network of Figure 16. The mistake was detected after

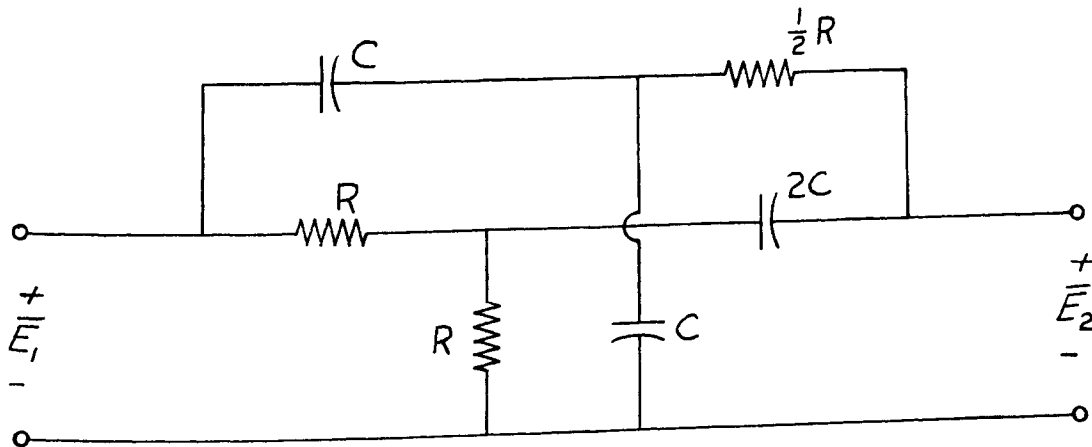


Figure 16. Diagram of a twin-tee filter with the output and common terminals interchanged.

a frequency-insensitive response was obtained. To explain the result, the circuit of Figure 16 was analyzed. It was found that

$$\frac{\bar{E}_2}{\bar{E}_1} = \frac{1}{2} \quad (10)$$

This then explained why the active filter response was not frequency dependent. Further analysis of the network yielded

$$\frac{\bar{E}_1}{\bar{E}_2} = \frac{j 4 \rho}{1 - \rho^2 + j 4 \rho} \quad (11)$$

No useful application is proposed for the expression of Eq. 10. The expression of Eq. 11 might be used as a lead-lag compensating network with zero attenuation and phase angle at  $\rho = 1$ .

APPENDIX I  
THE TWIN-TEE FILTER

A. BASIC THEORY

The twin-tee filter is a resistive-capacitive network which has the property of totally attenuating the output signal at some specified frequency. Figure 17 shows the circuit of this filter.

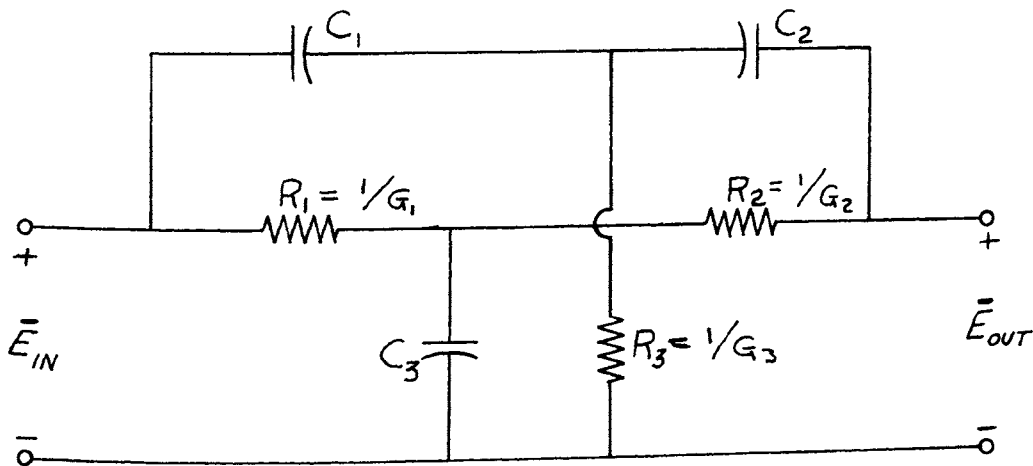


Figure 17. The twin-tee filter

An analysis of the circuit yields

$$\bar{\beta} = \frac{\bar{E}_{out}}{\bar{E}_{in}} = \frac{G_1 G_2 G_3 - \omega^2 C_1 C_2 (G_1 + G_2) + j\omega [G_1 G_2 (C_1 + C_2) - \omega^2 C_1 C_2 C_3]}{D} \quad (1)$$

where

$$D = G_1 G_2 G_3 - \omega^2 [C_1 C_2 (G_1 + G_2) + C_3 G_2 (C_1 + C_2) + C_2 C_3 G_3] + j\omega [G_1 G_2 (C_1 + C_2) + C_2 G_3 (G_1 + G_2) + C_3 G_2 G_3 - \omega^2 (C_1 C_2 C_3)] \quad (2)$$

Note that the numerator of the voltage transfer characteristic consists of real and imaginary parts, and that the real part vanishes at an angular frequency

$$\omega_r = \left[ \frac{G_1 G_2 G_3}{C_1 C_2 (G_1 + G_2)} \right]^{1/2} \quad (3)$$

and that the imaginary part vanishes at an angular frequency

$$\omega_i = \left[ \frac{G_1 G_2 (C_1 + C_2)}{C_1 C_2 C_3} \right]^{1/2} \quad (4)$$

In order that the real and imaginary parts of the numerator of  $\bar{\beta}$  vanish at the same value of  $\omega$ , it is necessary that

$$\frac{R_1 + R_2}{(R_1 + R_2)R_3} = \frac{C_1 + C_2}{C_3} = \frac{1}{n^2} \quad (5)$$

where  $n$  is some positive number. The number  $n$  shown above is the same as the number  $n$  used by Seeley and is equal to  $(n)^{-1/2}$  used by Valley and Wallman. If the relationships of Eq. 5 are substituted in Eq. 3 and 4, it is found that the numerator of Eq. 1 vanishes at an angular frequency

$$\omega_0 = \frac{1}{n} \left[ \frac{1}{R_1 R_2 C_1 C_2} \right]^{1/2} \quad (6)$$

and

$$R_3 = n^2 \left[ \frac{R_1 R_2}{R_1 + R_2} \right] \quad (7)$$

and

$$C_3 = n^2 [C_1 + C_2] \quad (8)$$

In order to make the selection of components easier and avoid confusion as to which is the input or output terminal pair, it is advantageous to make  $R_1 = R_2$  and  $C_1 = C_2$ , in which case

$$\omega_0 = \frac{1}{n R_1 C_1} \quad (9)$$

$$R_3 = \frac{1}{2} n^2 R_1 \quad (10)$$

$$C_3 = 2 n^2 C_1 \quad (11)$$

If the above expressions are substituted into Eq. 1, one then has

$$\bar{\beta} = \frac{1 - \left(\frac{\omega}{\omega_0}\right)^2}{1 - \left(\frac{\omega}{\omega_0}\right)^2 + j 2 \left(\frac{n^2+1}{n}\right) \left(\frac{\omega}{\omega_0}\right)} \quad (12)$$

or

$$\bar{\beta} = \frac{1 - \left(\frac{f}{f_0}\right)^2}{1 - \left(\frac{f}{f_0}\right)^2 + j 2 \left(\frac{n^2+1}{n}\right) \left(\frac{f}{f_0}\right)} \quad (13)$$



$$\bar{\beta} = \frac{1 - \rho^2}{1 - \rho^2 + j 2 \left(\frac{n^2+1}{n}\right) \rho} \quad (14)$$

where  $\rho = f/f_0$ . From the above expression, it can be seen that the value of  $\bar{\beta}$  is zero for  $\rho = 1$  and the value of  $\bar{\beta}$  approaches unity for very large and small values of  $\rho$ .

Figure 18 shows the variation of the phase and magnitude of  $\bar{\beta}$  versus frequency for  $n = 1$ .

It can be shown that optimum filter sharpness or minimum bandwidth is obtained when  $n = 1.16$ . In this case

$$\omega_0 = \frac{1}{R_1 C_1} \quad (15)$$

$$R_3 = \frac{1}{2} R_1 \quad (16)$$

$$C_3 = 2 C_1 \quad (17)$$

Eq. 12 then becomes

$$\bar{\beta} = \frac{1 - \rho^2}{1 - \rho^2 + j 4 \rho} \quad (18)$$

The above derivation was based on the assumption that the output load of the filter was an open circuit. If a load resistance  $R_L$  is connected to the output terminals, it is

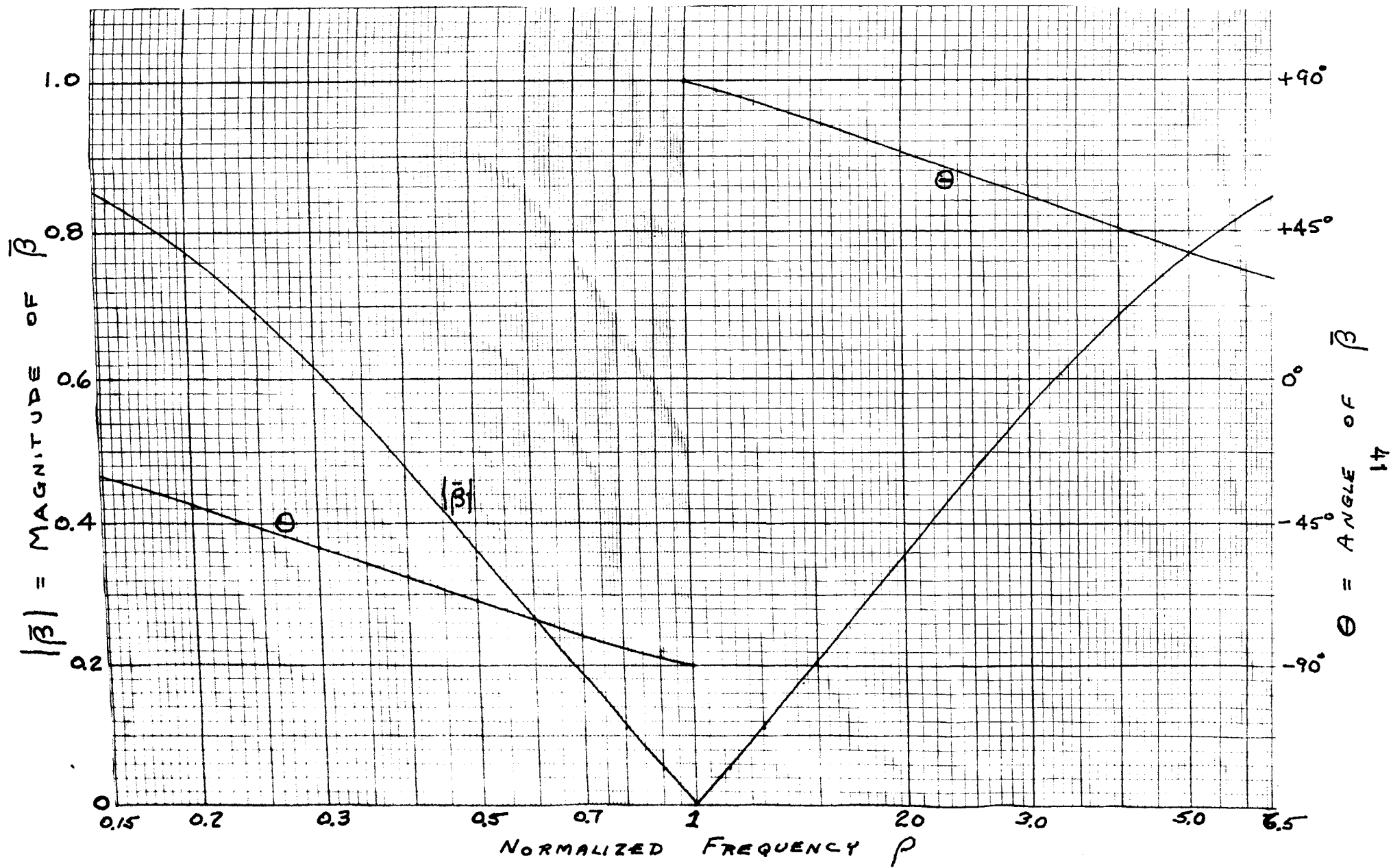


Figure 18. Frequency characteristics of a twin-tee filter with  $n=1$ .

found that

$$\bar{\beta} = \frac{1 - \rho^2}{(1 - \rho^2 + 2 R_1/R_L) + j\rho(4 + 2 R_1/R_L)} \quad (19)$$

Note that  $\bar{\beta}$  still vanishes at  $\rho = 1$ , but the sharpness of the filter is decreased.

For an open-circuit load, the input impedance is

$$\bar{Z}_{in}(j\omega) = \frac{R_1}{4} \left(1 + \frac{1}{j\rho}\right) + \frac{R_1}{2} \frac{1}{(1 + j\rho)} \quad (20)$$

and for  $\rho = 1$ ,

$$\bar{Z}_{in}(j\omega_0) = \frac{R_1}{2} (1 - j1) \quad (21)$$

For an input voltage source with zero internal impedance, the output impedance of the filter is,

$$\bar{Z}_{out}(j\omega) = \frac{2R_1(1 + j\rho)}{1 - \rho^2 + j4\rho} \quad (22)$$

and for  $\rho = 1$ ,

$$\bar{Z}_{out}(j\omega_0) = \frac{R_1}{2} (1 - j1) \quad (23)$$

#### B. TUNING TWIN-TEE FILTERS TO OBTAIN A SPECIFIED NULL AT A SPECIFIED FREQUENCY.

When constructing twin-tee filters, some means must be provided to compensate for component value variations. Even

with unequal component values, a relative null or minimum output will occur at some frequency close to the desired null frequency. Two degrees of freedom or variable components are required to obtain the desired null frequency and magnitude. These two degrees of freedom correspond to the frequencies at which the real and imaginary parts of the numerator of vanish (see Eq. 1, 3, and 4). One method described in the literature is based upon adjustment of resistances  $R_1$  and  $R_3$ .<sup>17</sup> This technique is more advantageous for thin-film networks where capacitors are not easily varied. The author obtained satisfactory filters by adjustment of  $R_3$  and  $C_3$ . In Eq. 3 note that  $\omega_r$  is independent of  $C_3$  and in Eq. 4,  $\omega_c$  is independent of  $R_3$ . This was used in the following manner. The circuit of Figure 19 was constructed and the oscillator frequency was adjusted to obtain a Lissajous pattern of a straight line (angle of  $\bar{\beta} = 0$ ). For an unbalanced filter,

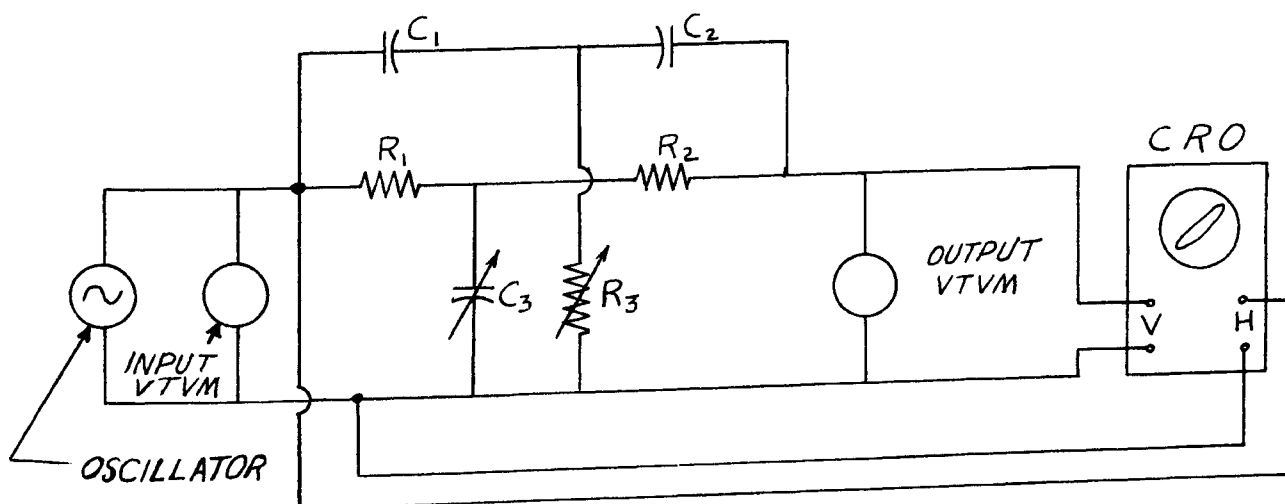


Figure 19. Circuit for tuning twin-tee filters

the slope of the Lissajous pattern is either positive or negative. This leads to four possible cases.

1. The slope is positive at a frequency less than that desired and the attenuation is not sufficient. The response may be improved by adding a resistance in parallel with  $R_3$ .

2. The slope is positive at a frequency greater than that desired and the attenuation is not sufficient. The response may be improved by adding a capacitor in parallel with  $C_3$ .

3. The slope is negative at a frequency less than that desired and the attenuation is not sufficient. The response may be improved by decreasing  $C_3$ .

4. The slope is negative at a frequency greater than that desired and the attenuation is not sufficient. The response may be improved by increasing  $R_3$ .

In the event the attenuation or the null frequency is satisfactory and the other is not, it is necessary to unbalance the filter further and then apply the above methods. This further unbalance should be effected to result in a positive slope. A satisfactory filter may then be easily obtained by the addition of parallel elements (increasing  $C_3$  or decreasing  $R_3$ ). Economic restrictions ruled out the use of adjustable components and it was necessary to balance the filters by substitution of discrete components with different values. The values of the compensating resistances were usually 10 times greater than  $R_3$ . The values of the compensating capacitors were usually less than one-tenth the value

of  $C_3$ . Figure 20 shows the construction of the filter boards in the equipment. The components to be adjusted,  $R_3$  and  $C_3$ , are in the center branches.

The circuit of Figure 19 was used to balance the filters, prior to the construction of the amplifiers. When all of the sections were assembled, it was observed that wiring capacitance caused a slight detuning of the filters for the higher frequencies. These filters were then retuned, using the circuit of Figure 21 and the procedure below.

1. The decade and band switches were set to connect the desired filter to an amplifier stage.
2. The 6SN7 for the stage was removed.
3. The 12AX7 grids (pin 7) for that stage and the following stage were connected to ground.
4. An input signal of the proper frequency was applied to terminal 3 of the 6SN7 socket.
5. The output signal was measured at terminal 1 of the 6SN7 socket and the components  $C_3$  and  $R_3$  were adjusted to obtain a minimum output voltage.

Note that the removal of the 6SN7 breaks the feedback path. This gives several advantages over the method discussed previously. These advantages are:

1. A smaller input signal and a less sensitive output detector are required, as the output of the twin-tee filter is amplified approximately 40 times before being measured by the output voltmeter. As the magnitude of the oscillator's output signal is reduced, the harmonic content of this signal

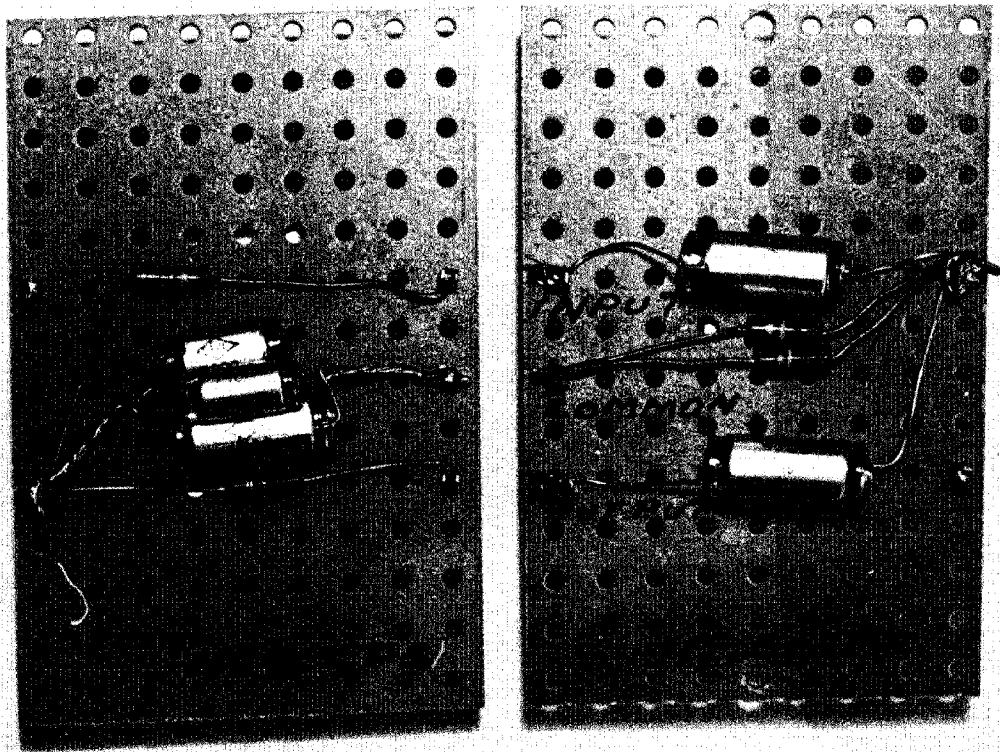


Figure 20. Construction of the twin-tee filter boards. The components  $R_3$  and  $C_3$  are in the center branches.

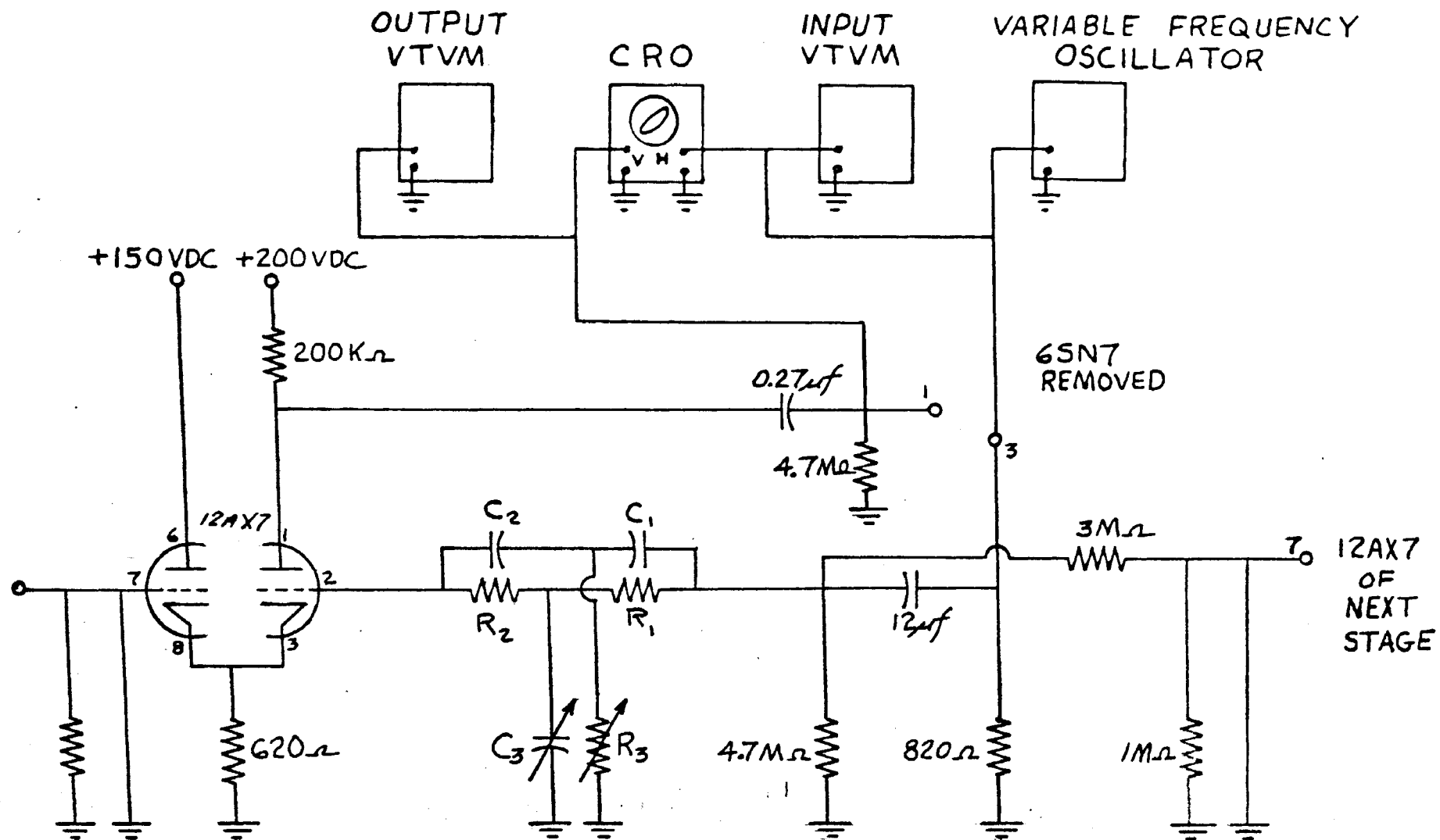


FIGURE 21. A CIRCUIT FOR TUNING THE TWIN-TEE FILTERS AFTER INSTALLATION.



is also greatly reduced. This results in a more purely sinusoidal signal. For example, assume the oscillator signal has 0.1% harmonic content for a 1 volt output. For an attenuation of 1000 at the null frequency, the fundamental and harmonic components of the filter's output signal have approximately equal magnitudes of 1 millivolt.

2. Except for the removed 6SN7 the circuit is the same as it would be in actual operation. Thus, all effects, such as wiring capacitance and phase shifts due to coupling networks, may be taken into account when balancing the filter.

The procedure for balancing the filters is the same as discussed previously, except that the slope of the Lissajous pattern is reversed, due to the phase inversion of the 12AX7.

## APPENDIX II

### OPERATING, MODIFICATION, AND MAINTAINANCE INSTRUCTIONS

#### A. OPERATING INSTRUCTIONS

When preparing to process signals, the equipment should be turned on at least 15 minutes prior to making measurements. This allows the transient effects to decay.

The input and output terminals are labeled, red jacks at the left side of the front panel (see Figure 6). The black jacks below the input and output jacks are connected to the circuit ground. The circuit ground is connected to the metal skin of the box and to the ground (white) conductor of the 110 volt 60 cps power cord. The 60 cps noise in the equipment's output signal will be greatly reduced if a good ground is provided at the 60 cps power supply.

The frequency range or decade of interest is selected first, by the decade switch. The particular frequency band is then selected by the band switch. The pilot lights above each band switch will indicate which decade is being used, even if the bundles of connecting cables are interchanged by mistake.

The response of the equipment is linear for input signals having a magnitude of 200 mv or less inside any frequency band. This corresponds to an output signal of approximately 0.8 volt. If it is desired to process larger signals, the equipment must be modified. Suggested methods of modification are given in the following section.

## B. MODIFICATION OF THE EQUIPMENT

When making the final adjustments to the equipment prior to delivery, the values of several components and bias voltages were changed to provide satisfactory performance with the expected signal level. In the event that the equipment is required to process larger or smaller signal levels in the future, several simple changes should be made for best performance. These changes are discussed below.

### 1. Changes to provide for larger input signals.

This modification is quite easily done by connecting a resistance  $R$  between the input jack and the terminal of the signal source as shown in Figure 22.

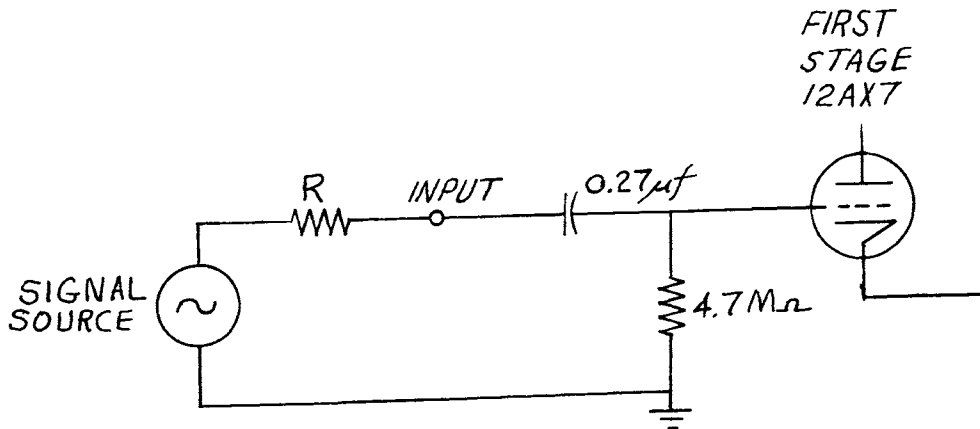


Figure 22. Modification for larger input signals.

The resulting output is then reduced by the factor  $4.7 \text{ m}\Omega / (4.7 \text{ m}\Omega + R)$ . It is possible that this connection might result in a large amount of 60 cps noise. In this event, the resistance  $R$  should be placed close to the  $4.7 \text{ m}\Omega$  resistance inside the box.

### 2. Changes to provide for smaller input signals.

In the event that the output signal is too small, changes

must be made to the circuit inside the box. The output of each stage is now attenuated by a factor of 4 before being applied to the following stage. The attenuation is due to resistive voltage-dividers (see  $R_7$  and  $R_8$  in Figure 5). The voltage dividers consist of  $3\text{ m}\Omega$  and  $1\text{ m}\Omega$  resistances. The output may be increased by replacing the  $3\text{ m}\Omega$  resistance with a smaller resistance  $R$ . The resulting output signal is increased by a factor of  $4\text{ m}\Omega/(1\text{ m}\Omega + R)$ , for each of the voltage dividers so modified. In no case should the output signal be larger than one volt for linear operation. Two 6SN7 triode units are not now used, but are available for signal amplification if desired.

#### C. MAINTAINANCE

It is expected that this equipment should require little maintainance, other than the replacement of vacuum tubes and pilot light bulbs. Several other possible sources of trouble are discussed below. To simplify maintainance, the following procedures should be used.

1. Pilot lamp replacement. The pilot lights use General Electric type 1847 bulbs and the bulbs may be replaced by unscrewing the plastic caps on the front panel. This may be done without removing the front panel.

2. Amplifier tube replacement. It is suggested that the military industrial versions of the tubes be used for replacement. These tube numbers are 5751 and 6SN7WGT. Both these tubes have parallel heater elements and a visual examination may not detect the failure of one heater element. The

exchange of tubes is most quickly done by removing the back panel.

3. Fuse replacement. The 1.5 amp fuse is located on the power supply chassis and is replaced by removing the back panel.

4. General amplifier maintainance. Figure 23 shows the schematic diagram of the amplifier circuits. Tube failures or amplifier malfunctions may be located by measuring the D.C. voltages indicated on the diagram. The D.C. voltages were measured with a vacuum-tube voltmeter. The aluminum chassis is the circuit ground. Figure 24 shows the amplifier rack. The power supply chassis is located on the left and the amplifier chassis on the right. Various points and sections of the circuit are identified with colored tags. When making amplifier measurements, the cable connectors must be in place. Otherwise, the grids of the 12AX7's are not connected to the circuit.

5. Power supply maintainance. Figure 25 shows the schematic diagram of the power supply, with D.C. voltage readings. Most of the components are operated at less than half their rated voltages or currents and should give little trouble. The most likely source of trouble is the OD3 (150v) voltage regulator tube. Due to aging, the breakdown voltage will increase with time and the current through the tube will decrease from the desired value of 25 milliamperes. If the OD3 voltage increases sufficiently, oscillations will occur in the amplifier sections. The identification and prevention

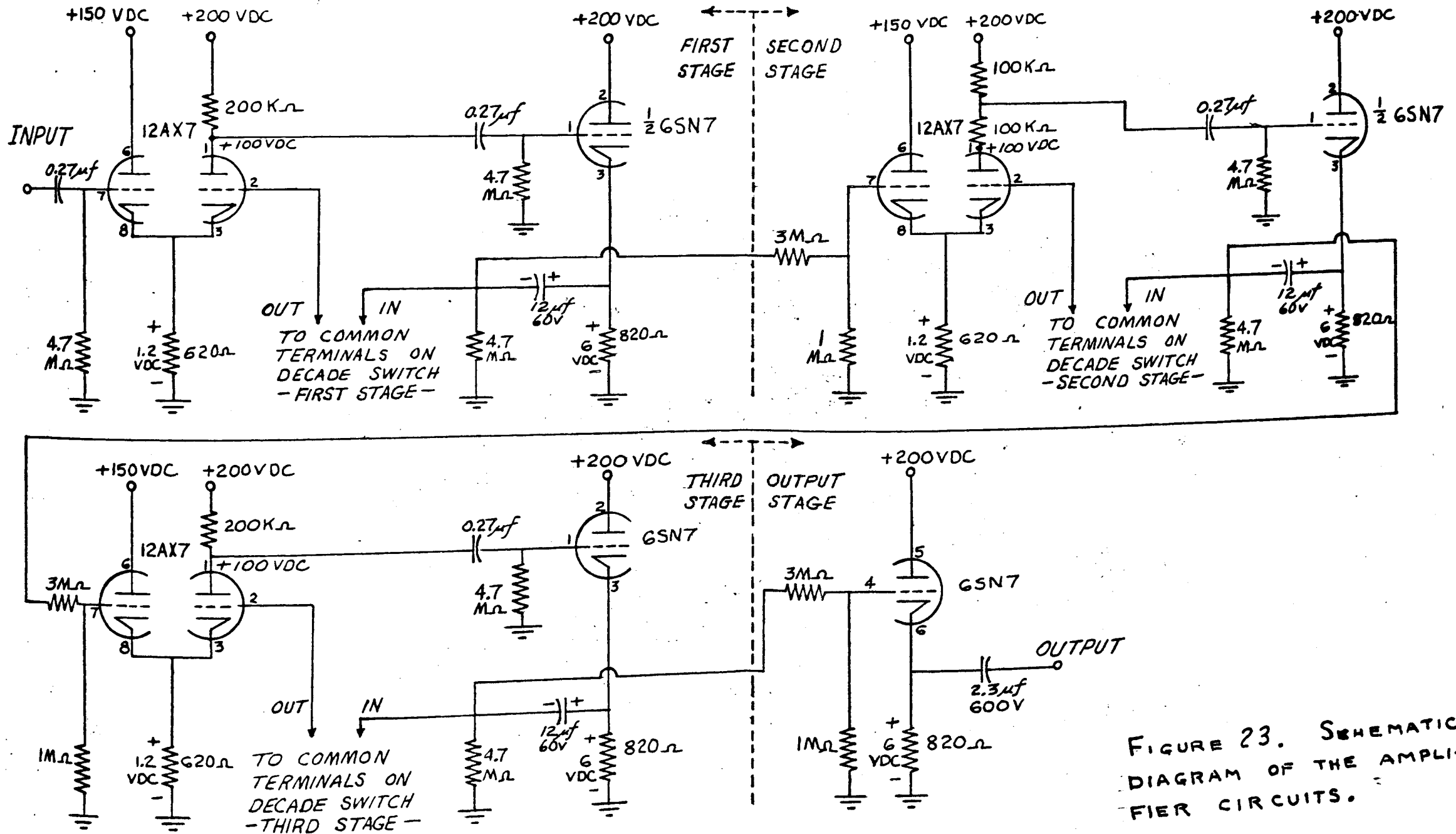


FIGURE 23. SCHEMATIC DIAGRAM OF THE AMPLIFIER CIRCUITS.

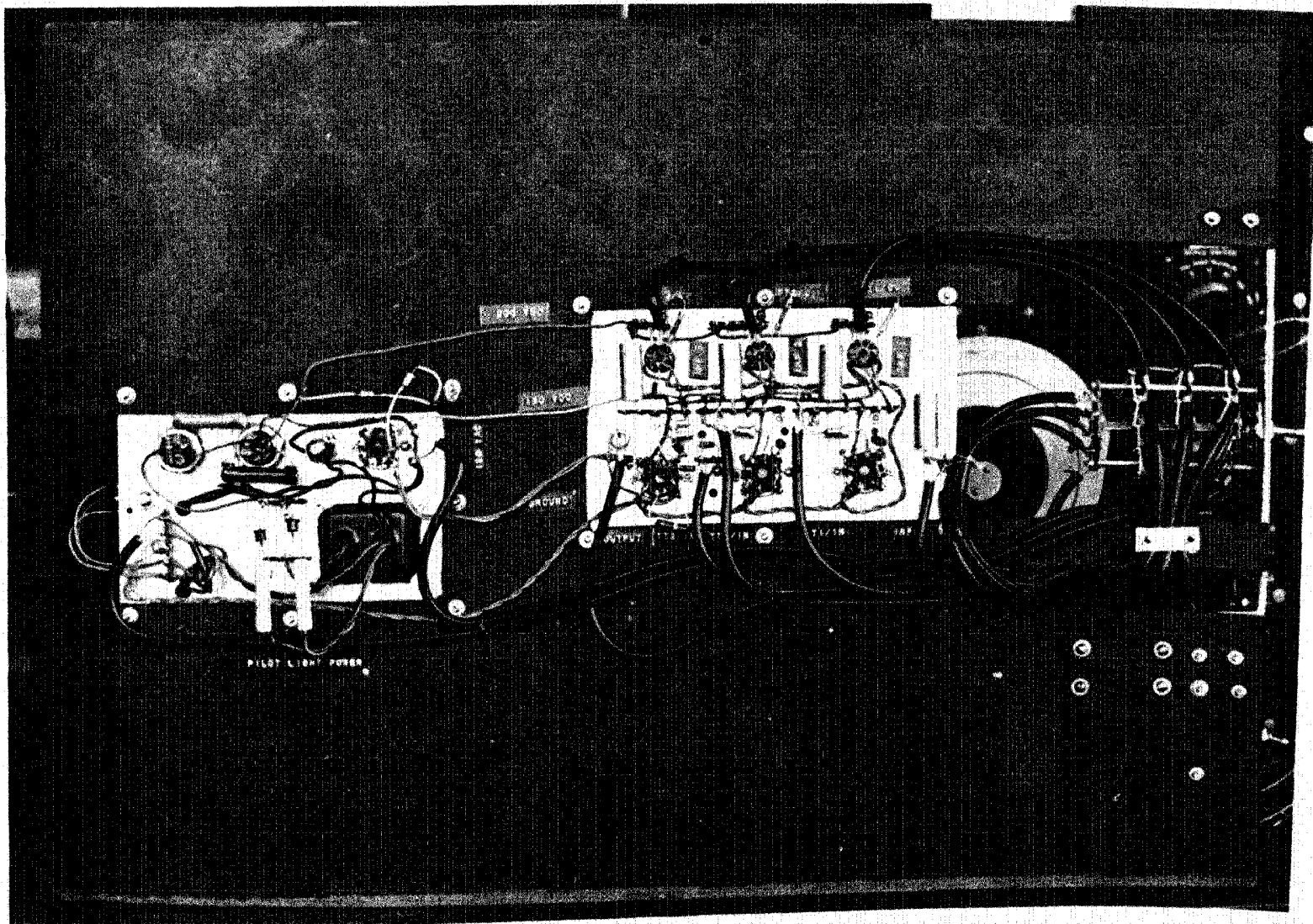


Figure 24. Rear view of the amplifier rack.

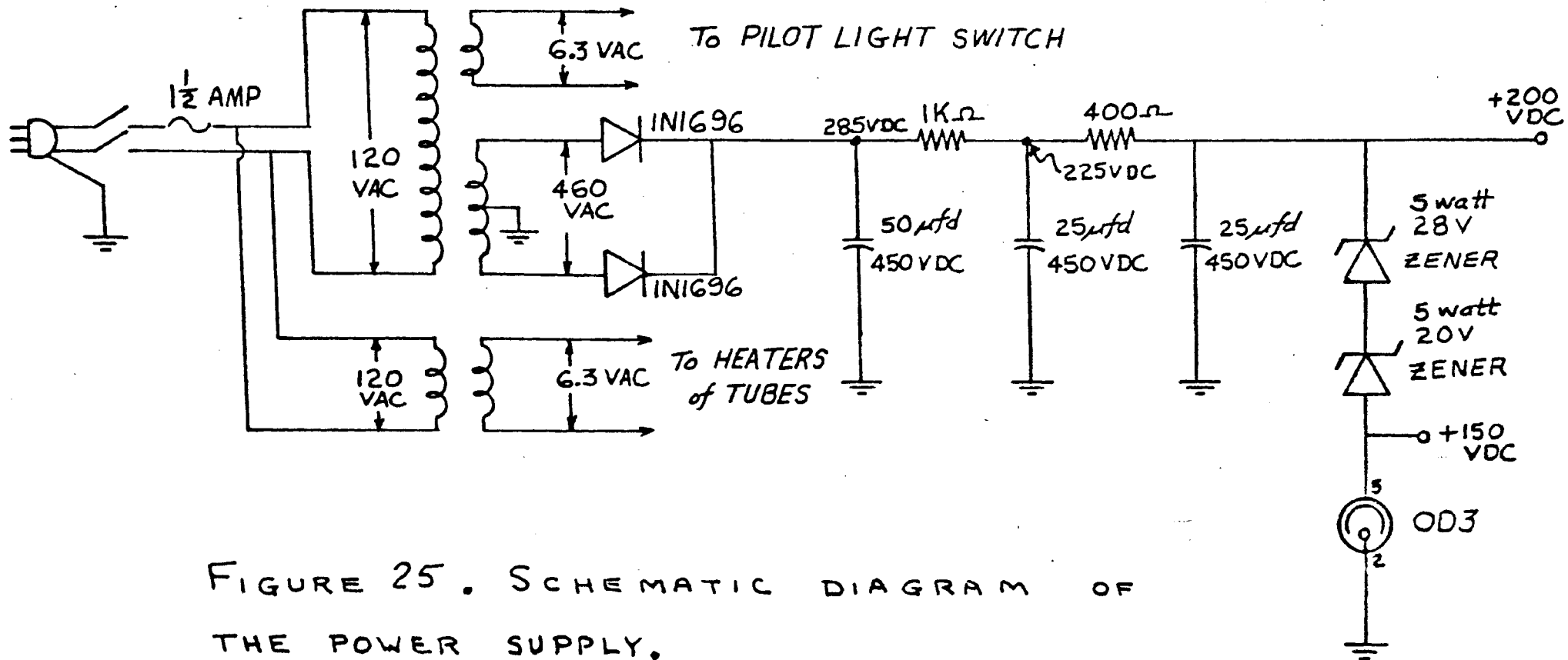


FIGURE 25. SCHEMATIC DIAGRAM OF THE POWER SUPPLY.



of these oscillations is discussed below.

6. Oscillations. Two possible sources of oscillation are present in the equipment. The first source arises from an interaction of the power supply and amplifier sections. The second source is due to large changes in the values of the components in the twin-tee filters. The characteristics and appropriate remedies for both sources of oscillation are presented below.

(a) Oscillations due to the power supply. These oscillations are characterized by a change in frequency of oscillation each time a band or decade switch is changed. Another symptom is a flickering, rather than a steady glow, in the OD3 tube. When a switch position is changed, the grid (pin 2) circuits of the 12AX7 tubes are open-circuited momentarily. This causes a surge of current through these tubes. If the surge current is greater than the D.C. power supply can deliver and still maintain 150 volts across the OD3 tube, the OD3 glow will extinguish. The plate-supply voltage drops suddenly and the equivalent of a voltage pulse is applied to the circuit. The power supply and the filter stages, each with its own frequency characteristic, form an unstable feedback system. For a given band position, oscillations will occur at a frequency approximately equal to the band-center frequency of the next highest frequency band. Oscillations occur at this frequency (outside the band for that switch position) because the total phase angle imparted by the three cascaded filter stages is  $180^\circ$  (lagging)

at this frequency. The signal occurring at the grid of the 6SN7 output tube has the proper phase and magnitude to reinforce, via the power supply, the signal at the first amplifier stage. Oscillations are prevented by including sufficient surge current capacity in the D.C. power supply. A current of 25 milliamperes through the OD3 tube is quite sufficient, as these oscillations do not occur for OD3 current greater than 12 milliamperes. Due to the effects of aging, the OD3 current will decrease and oscillations may eventually occur. The oscillations may be stopped by replacing the OD3 tube or by reducing resistances ( $1\text{ k}\Omega$  and  $400\Omega$ ) in the power supply. Replacement of the tube is preferred.

(b) Oscillations due to faulty twin-tee filters. These oscillations are caused by large changes in filter component values. The oscillations will occur for one or at most two adjacent band switch positions (the frequency of oscillation being the same for the case of two switch positions). The oscillations are stopped by repairing or replacing the faulty twin-tee filter. To find the faulty filter, note the decade and band switch positions and the stage in which the oscillations originate. The decade switch position will indicate the filter rack to be repaired. Figure 31 (in a following section) shows the filter connections at a band switch. The band switch position determines the filter connected to the stage in which the oscillations originate. The actual location of the filter on the rack is determined by using Figure 33 (also in a following section). For example, oscillations

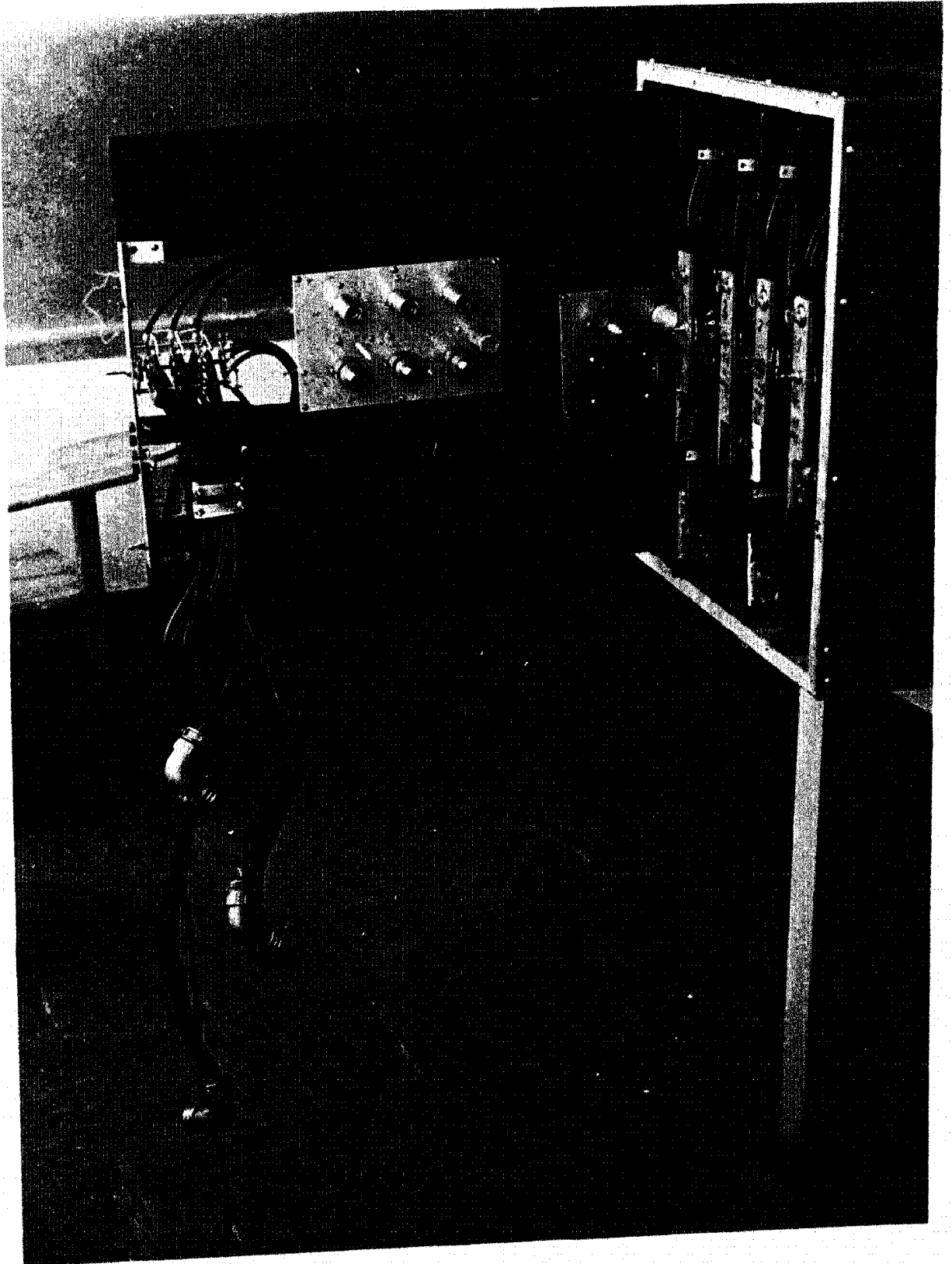
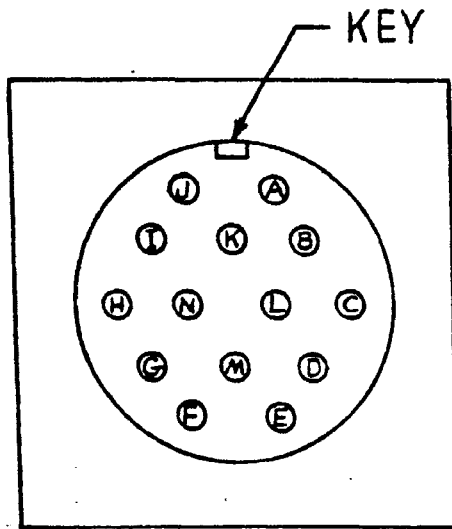


Figure 26. Front view of the amplifier rack.

BACK VIEW



<u>Pin</u>	<u>Connection</u>
A	filter 2 output
B	filter 3 input
C	filter 3 output
D	ground
E	pilot light
F	pilot light
G	ground
H	filter 1 input
I	filter 1 output
J	filter 2 input
K	ground
L	ground
M	no connection
N	ground

Figure 27. Rear view of a connector plug and wiring details.

for racks 2 and 3 should then be exchanged. With the decade switch on position 3, the filters for rack or decade 2 will then be connected to the amplifier stages. This will be indicated by the pilot light on rack 2.

Figure 28 shows the signal path through a twin-tee filter for a set of decade and switch positions. Figure 29 shows the details of the decade switch connections. Figures 30 and 31 show the details of a typical band switch. The input and output designations refer to the input and output of the twin-tee filters. The use of these diagrams is explained on pages 57-58.

9. Location of the twin-tee filters on the rack.

Figures 32 and 33 show a typical rack viewed from the same side. In Figure 33, the squares represent the filters and the number in each square indicates that filter's null frequency.

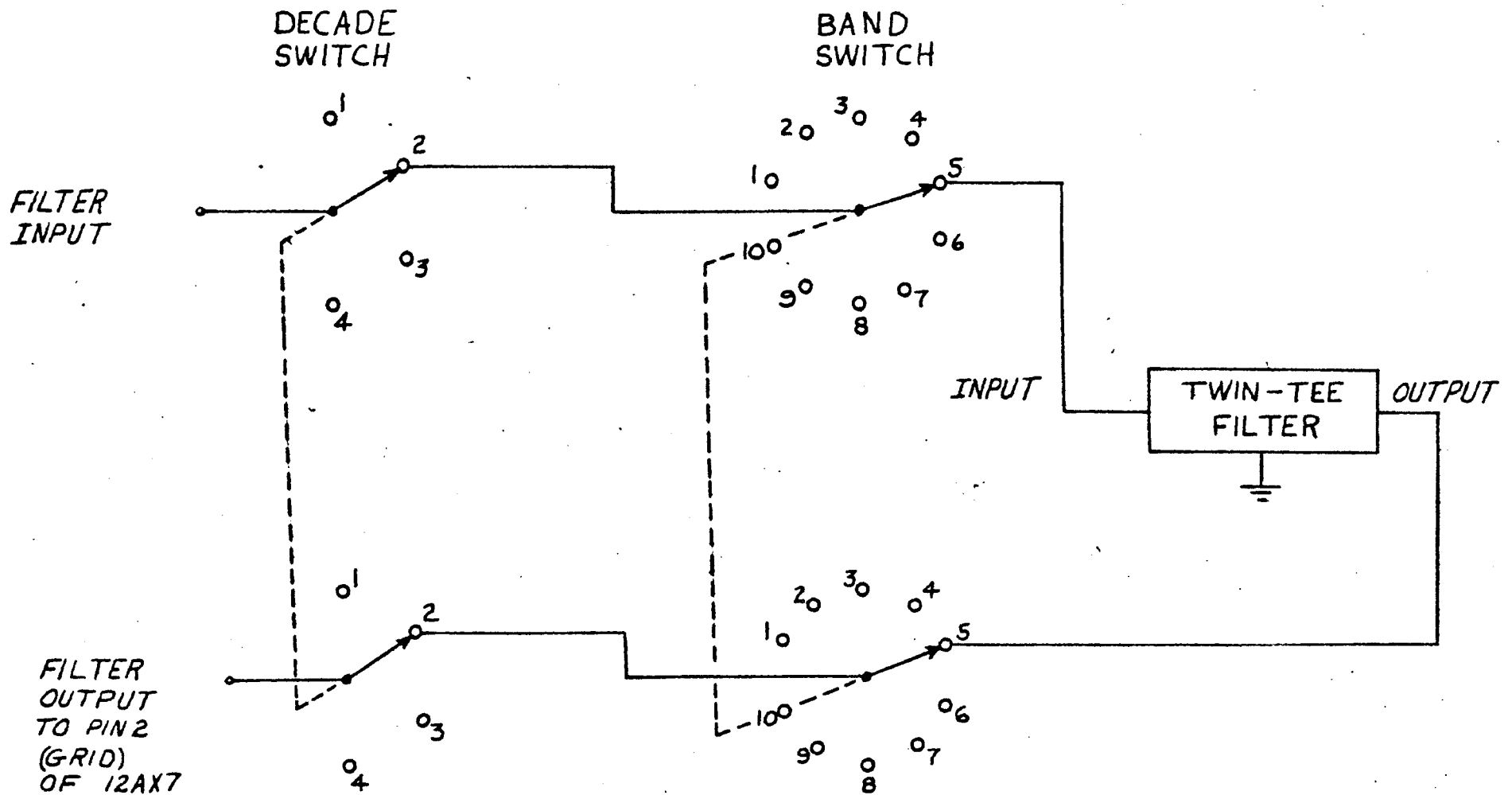
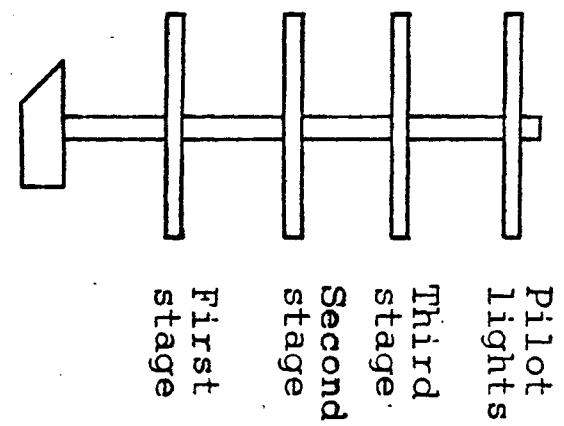
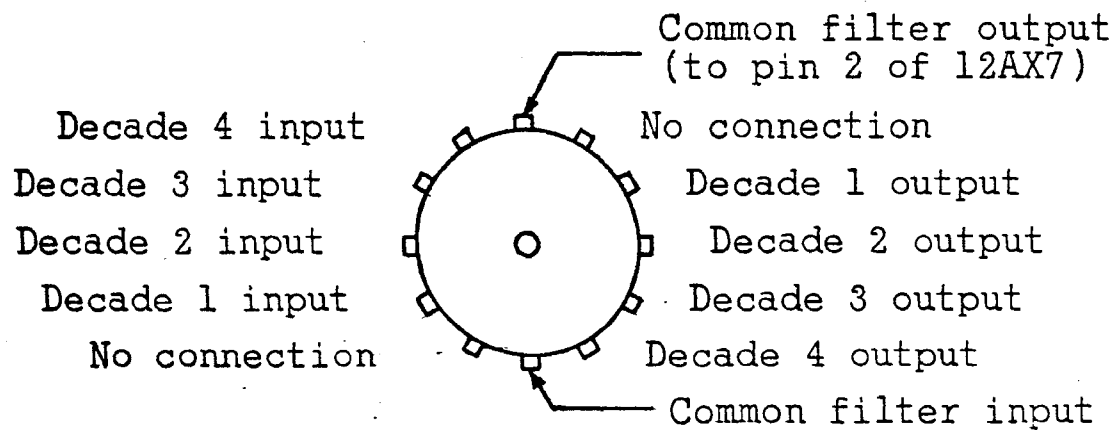


FIGURE 28. SIGNAL PATH THROUGH A TWIN-TEE FILTER.

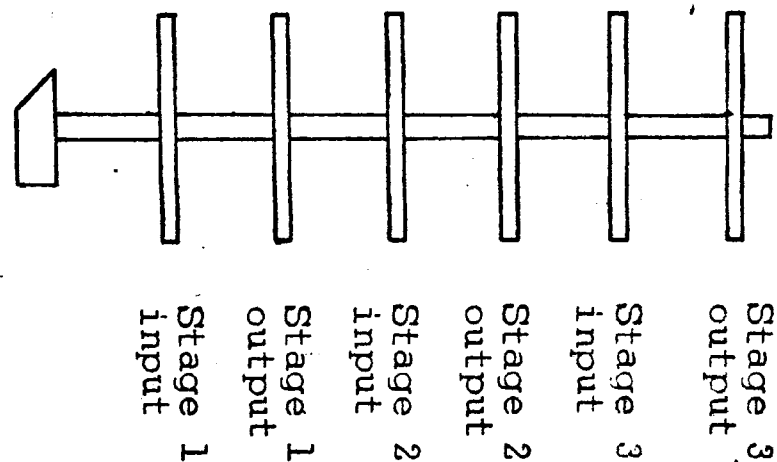
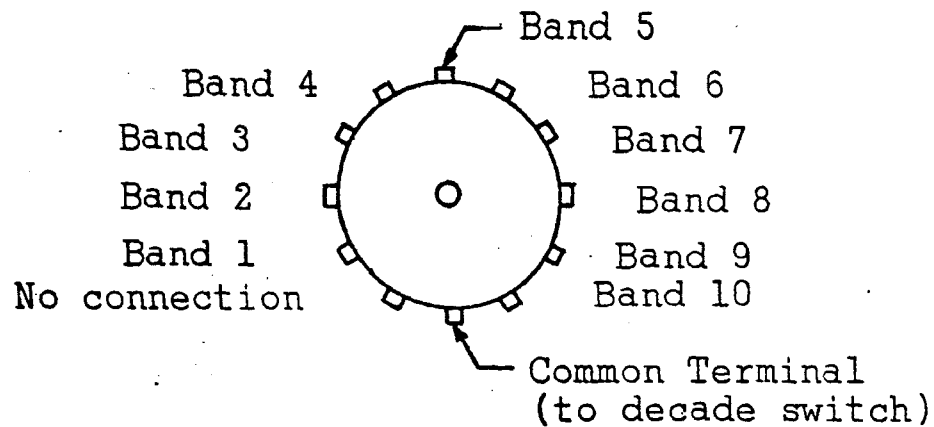


A Front View--The decade terminals are connected to the common terminals on the band switches.

B Side View

**FIGURE 29.**

Details of the Decade Switch that is Mounted on Amplifier Rack



A Front View--The band terminals are connected to the input and output terminals of the twin-tee filters.

B Side View

### FIGURE 30

Details of a Typical Band Switch that is Mounted on Filter Rack



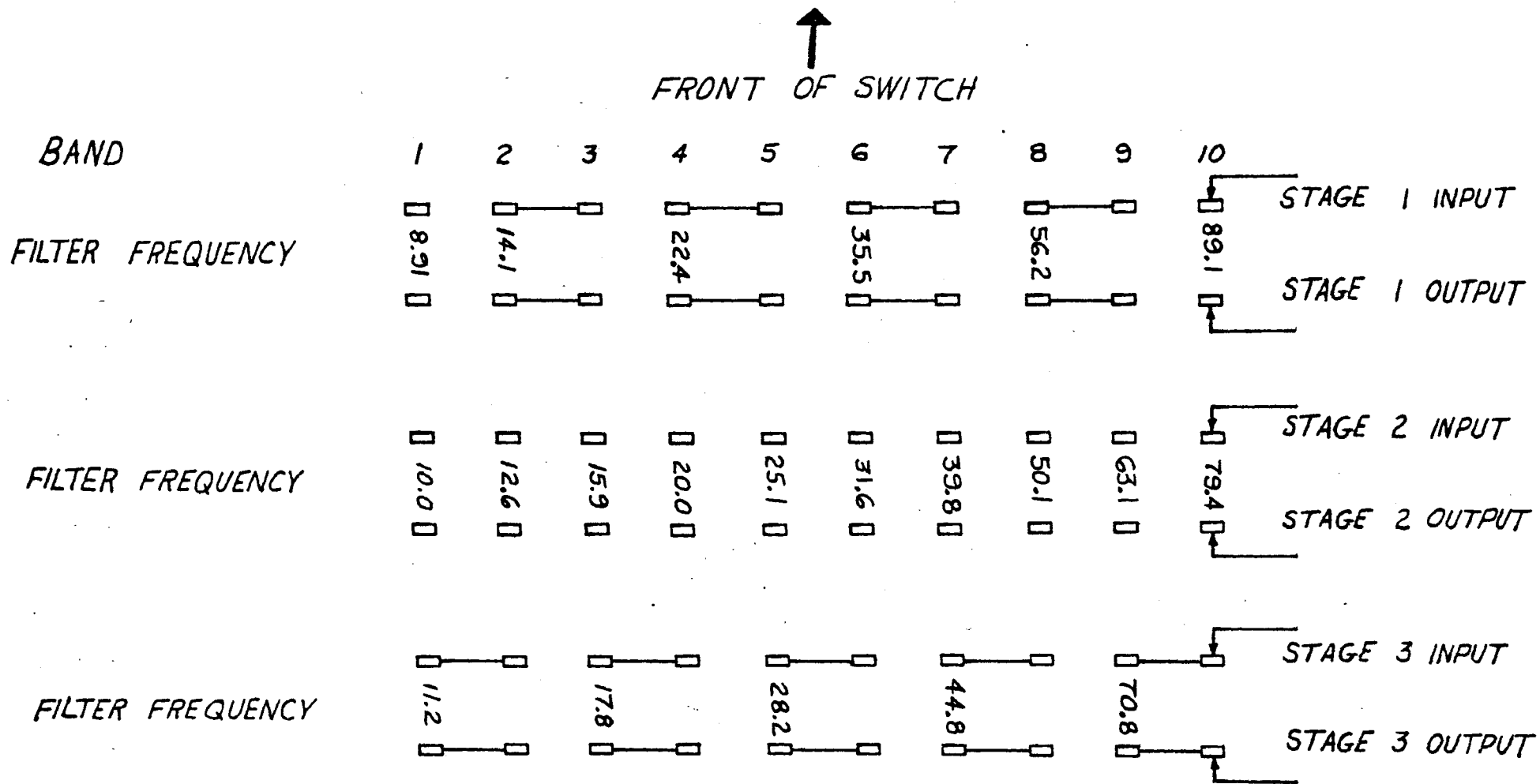


Figure 31. Details of the twin-tee filter connections to a band switch. The number between each terminal pair indicates the null frequency of the filter connected to that terminal pair.

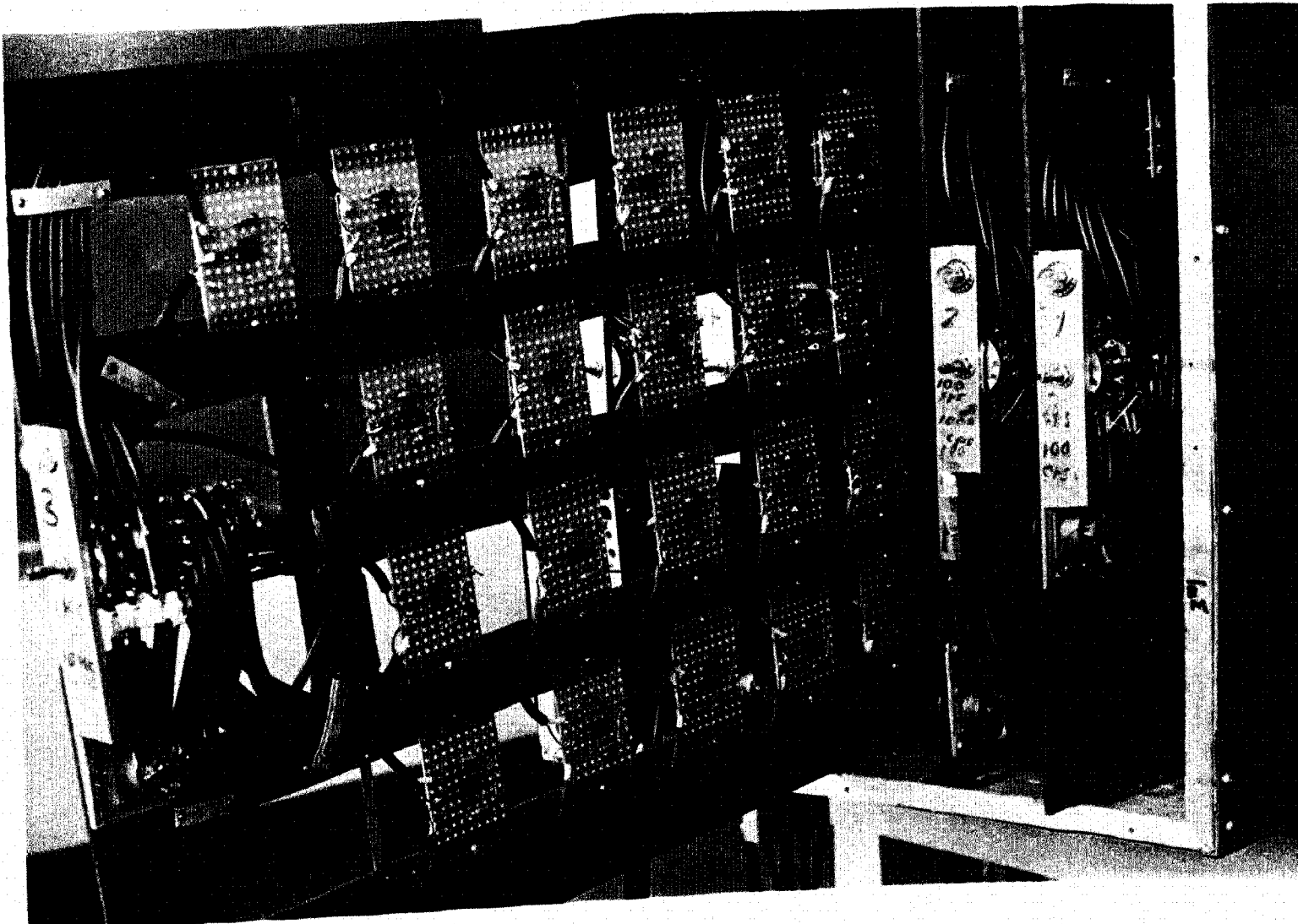


Figure 32. A view of a filter rack showing the filter board arrangement. Also see Figure 33.

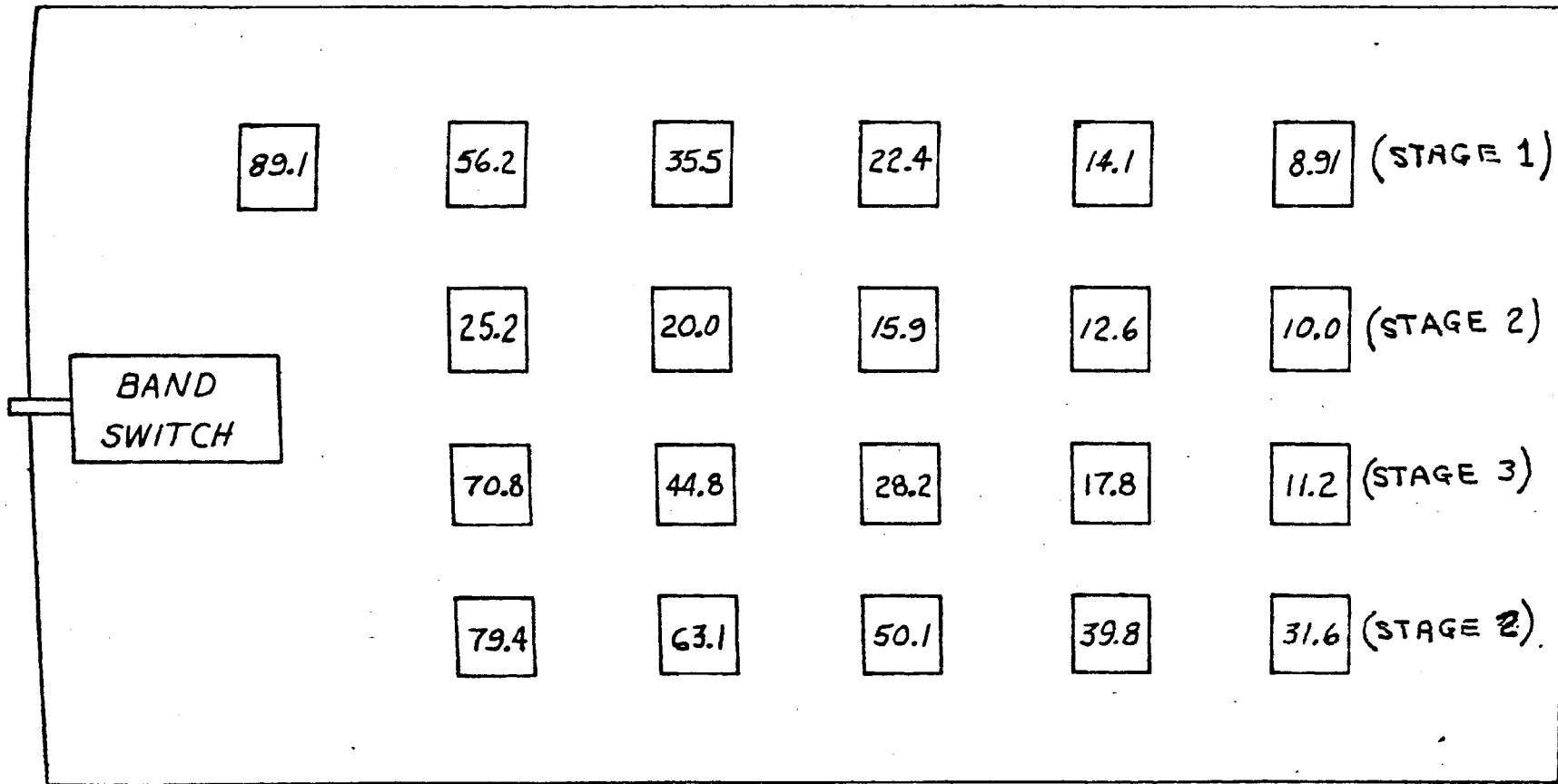


Figure 33. Arrangement of the filter boards on a filter rack. The number in each square indicates the null frequency of that twin-tee filter. Note that the filters for each stage are grouped by rows. The top terminal on each filter is the input, the center terminal is the common or ground, and the bottom terminal is the output terminal.

APPENDIX III  
DEFINITIONS OF BANDWIDTHS

In the experimental analysis of random signals, several frequency bandwidths have been used. Some of the more common designations are constant bandwidth filters, octave filters, one-third octave filters, and one-tenth decade filters.

For constant bandwidth filters, the band-pass frequency range is a fixed number of cycles per second, such as 10 cps or 100 cps, regardless of the band center frequency.

For octave filters, the center frequency of each band is twice the center frequency of the next lowest band. This common edge of two adjacent bands is fixed at the geometric mean of the two band-center frequencies.

For all practical purposes one-third octave filters and one-tenth decade filters are equivalent. The major difference is the manner in which the critical (lower-edge, band-center, and upper-edge) frequencies are computed to obtain approximately the same results. For one-third octave filters, the ratio of each band-center frequency to the next lowest band-center frequency is  $2^{1/3}$  (= 1.260). For one-tenth decade filters, the ratio of each band-center frequency to the next lowest band-center frequency is  $10^{0.1}$  (= 1.259). Since the band edges are also placed at the geometric means of the band-center frequencies, all the critical frequencies  $f_n$  may be found by

$$f_n = f_i (10)^{0.05 n} \quad (1)$$

where  $n = 1, 2, 3, \dots$  and  $f_i$  is a convenient value. Table 1 shows the critical frequencies for one decade with a bandwidth of one-tenth decade.

Band	Lower Band-Edge Frequency	Band-Center Frequency	Upper Band-Edge Frequency
1	8.91	10.0	11.2
2	11.2	12.6	14.1
3	14.1	15.9	17.8
4	17.8	20.0	22.4
5	22.4	25.1	28.2
6	28.2	31.6	35.5
7	35.5	39.8	44.8
8	44.8	50.1	56.2
9	56.2	63.1	70.8
10	70.8	79.4	89.1

Table 1. Critical frequencies for band-pass filters with bandwidths of one-tenth decade.

In the analysis of random processes such as turbulence, octave or decade type filters are generally used. These types of filters are preferred because the signal level is usually expected to decrease with increasing signal frequency. The

bandwidth (in cps) increases as the band-center frequency increases and tends to compensate for the reduced signal level per single frequency. The bandwidth of one-third octave results from a compromise between frequency resolution and the number of filters required.

END NOTES

<sup>1</sup>J. K. Vennard, Elementary Fluid Mechanics, (New York: John Wiley and Sons, Inc., 1962) pp. 226-229.

<sup>2</sup>J. O. Hinze, Turbulence, (New York: McGraw-Hill Book Co., 1959)

<sup>3</sup>Instruction manual for Disa type 55A01 Constant Temperature Anemometer, (Denmark: Disa Electronics, June 1963)

<sup>4</sup>J. G. Truxal, Control System Synthesis, (New York: McGraw-Hill Book Co., 1955) pp. 444-453.

<sup>5</sup>Ibid., p. 453.

<sup>6</sup>Ibid., p. 412.

<sup>7</sup>Ibid., pp. 443-444

<sup>8</sup>Disa Instruction Manual, loc. cit.,

<sup>9</sup>S. Seely, Electron Tube Circuits, (New York: McGraw-Hill Book Co., 1958) pp. 356-362.

<sup>10</sup>G. E. Valley and H. Wallman, Vacuum Tube Amplifiers, (New York: McGraw-Hill Book Co., 1948) pp. 384-408.

<sup>11</sup>Seely, loc. cit., p. 362.

<sup>12</sup>Ibid., p. 361.

<sup>13</sup>Valley and Wallman, loc. cit., pp. 407-408.

<sup>14</sup>Seely, loc. cit., p. 360.

<sup>15</sup>RCA Receiving Tube Manual, (Harrison, New Jersey: Radio Corporation of America, 1964)

<sup>16</sup>Valley and Wallman, loc. cit., p. 388.

<sup>17</sup>Electronics Products Magazine, (Garden City, New York: Tech Publishers, Inc., vol. 7, no. 1, pt. B, June 1964) pp. 52-53.

## VITA

The author was born on August 30, 1939 in Brewton, Alabama. He attended the primary and secondary schools in Flomaton, Alabama.

In September 1957, he entered Auburn University and received the Bachelor of Science Degree in Electrical Engineering in March 1962.

The author has been enrolled in the Graduate School of the University of Missouri at Rolla since September 1962.

During the summers of 1961-1964, he has been employed by the Chemstrand Company in Pensacola, Florida.

12/11/62